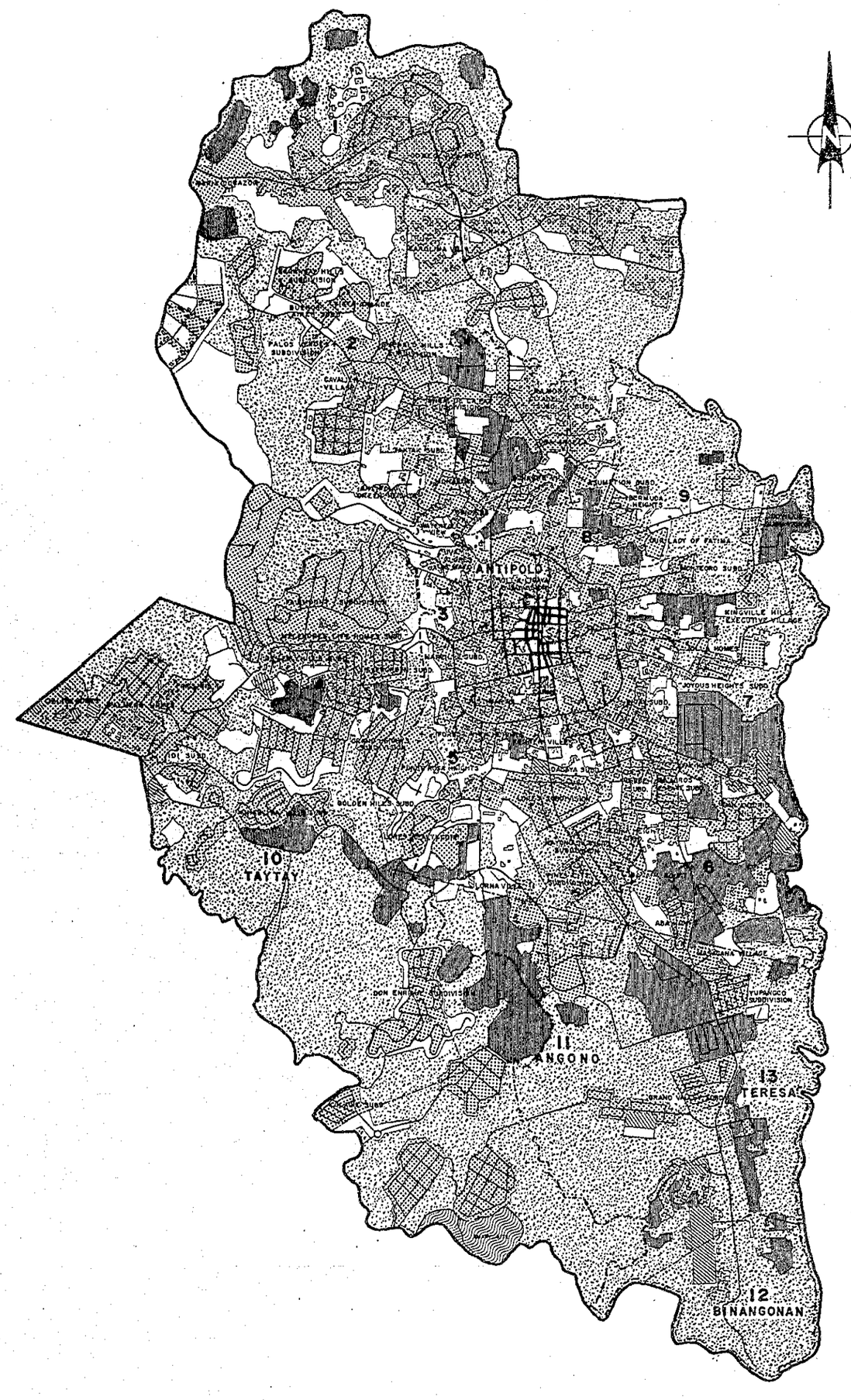

BARANGAY / MUNICIPALITY

1. Bagong Nayon
2. Sta. Cruz
3. De la Paz
4. Beverly Hills
5. San Roque
6. Dalig
7. San Jose
8. San Isidro
9. San Luis
10. Taytay
11. Angono
12. Binangonan
13. Teresa

STUDY AREA
AQUIFER BASIN ZONE
MUNICIPALITY BOUNDARY
BARANGAY BOUNDARY

SCALE 1:20,000

LEGEND

- BUILT-UP AREA
- COMMERCIAL AREA
- INDUSTRIAL AREA
- AGRICULTURAL LAND
- FOREST GRASS LAND
- OPEN SPACE
- OTHERS

STUDY FOR THE GROUNDWATER DEVELOPMENT IN METRO MANILA

JAPAN INTERNATIONAL COOPERATION AGENCY

FIGURE 6.1.77

FUTURE LAND USE MAP, ANTIPOLO AREA: 2010

ESTIMATED AREA BY LAND CATEGORY
ANTIPOLO AREA (1991)

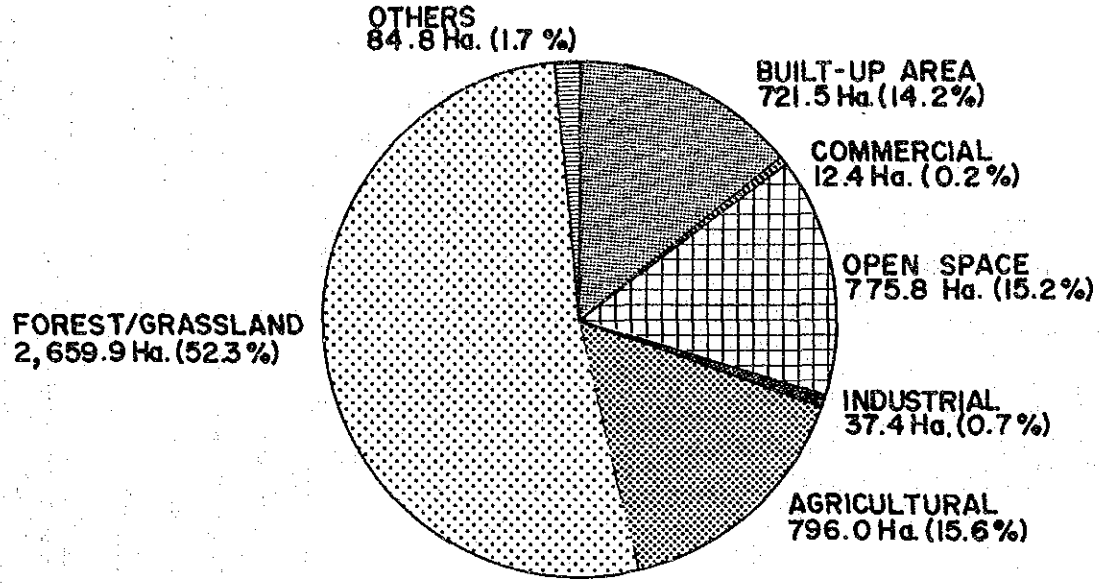

ESTIMATED AREA BY LAND CATEGORY
ANTIPOLO AREA (2010)

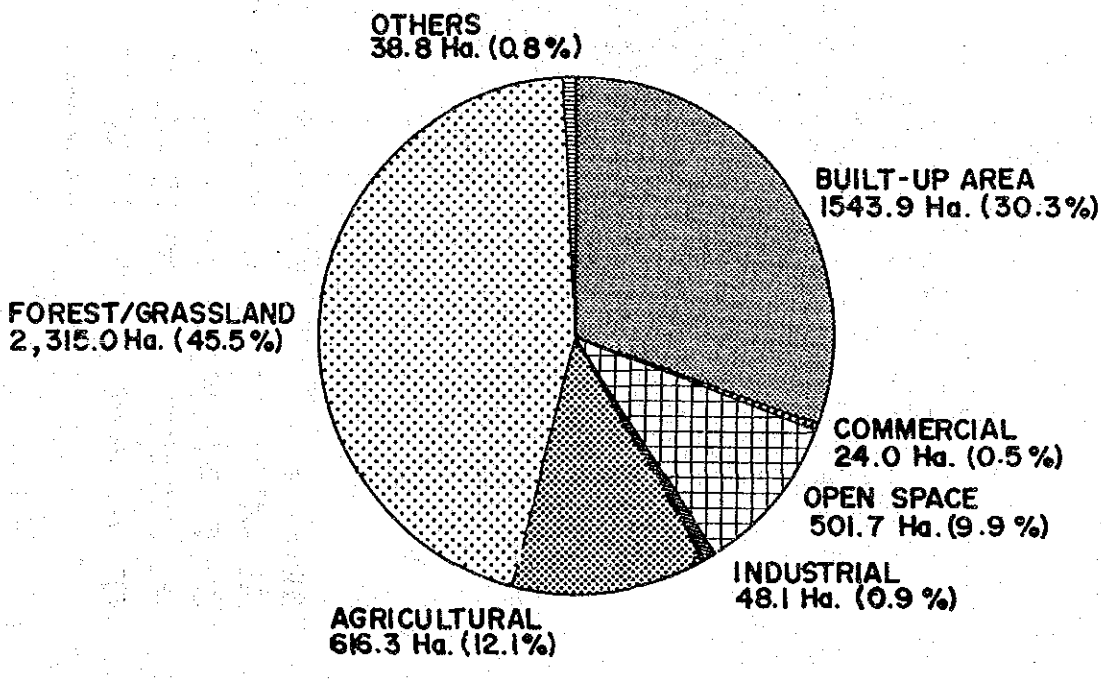

STUDY FOR THE GROUNDWATER DEVELOPMENT IN METRO MANILA JAPAN INTERNATIONAL COOPERATION AGENCY	FIGURE 6.1.8 LAND AREA COMPARISON, 1991-2010

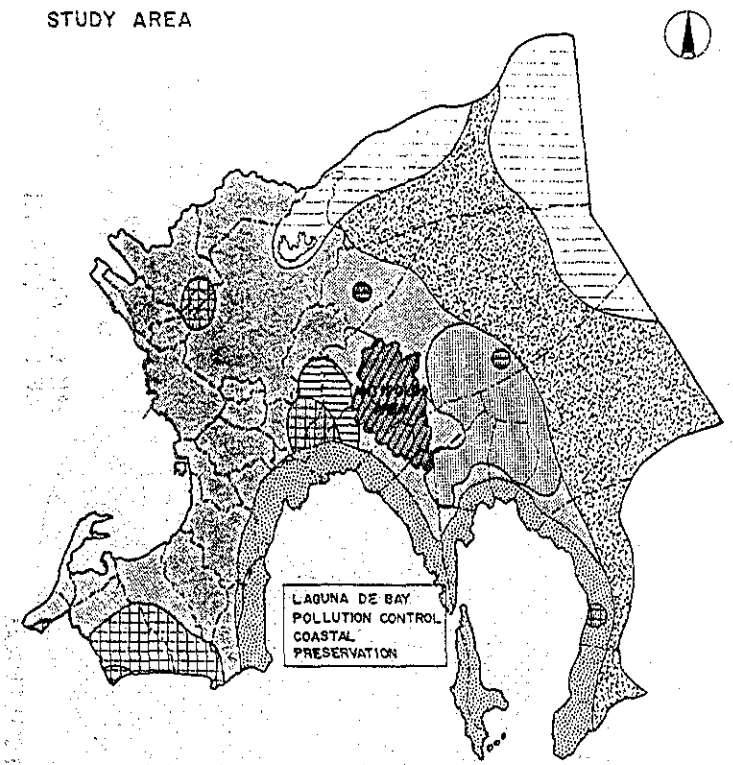

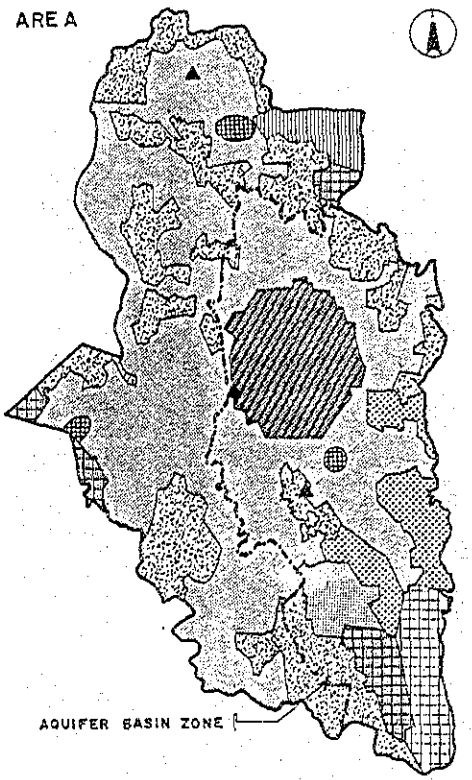

ANTIPOLO AREA
URBAN CONSOLIDATION ZONE
COMPLEMENTARY URBAN SATELLITES
FARMING & REGIONAL OPEN SPACE
AGRO- INDUSTRIAL
EXISTING INDUSTRIAL AREA
PROPOSED INDUSTRIAL AREA
GREEN BELT
PRESERVATION AREA (FOREST AREA)
PRESERVATION AREA (WATERSHED)
FLOODING AREA

RESIDENTIAL AND COMMERCIAL
RESIDENTIAL
RESETTLEMENT AREA
COMMERCIAL
INDUSTRIAL
GREEN AREA
AGRICULTURE
AGRO- INDUSTRIAL
OPEN SPACE (FUTURE RESIDENTIAL DEVELOPMENT)
TOURIST POINT

STUDY FOR THE GROUNDWATER DEVELOPMENT IN METRO MANILA
JAPAN INTERNATIONAL COOPERATION AGENCY

FIGURE 6.1.9
LAND USE PLAN

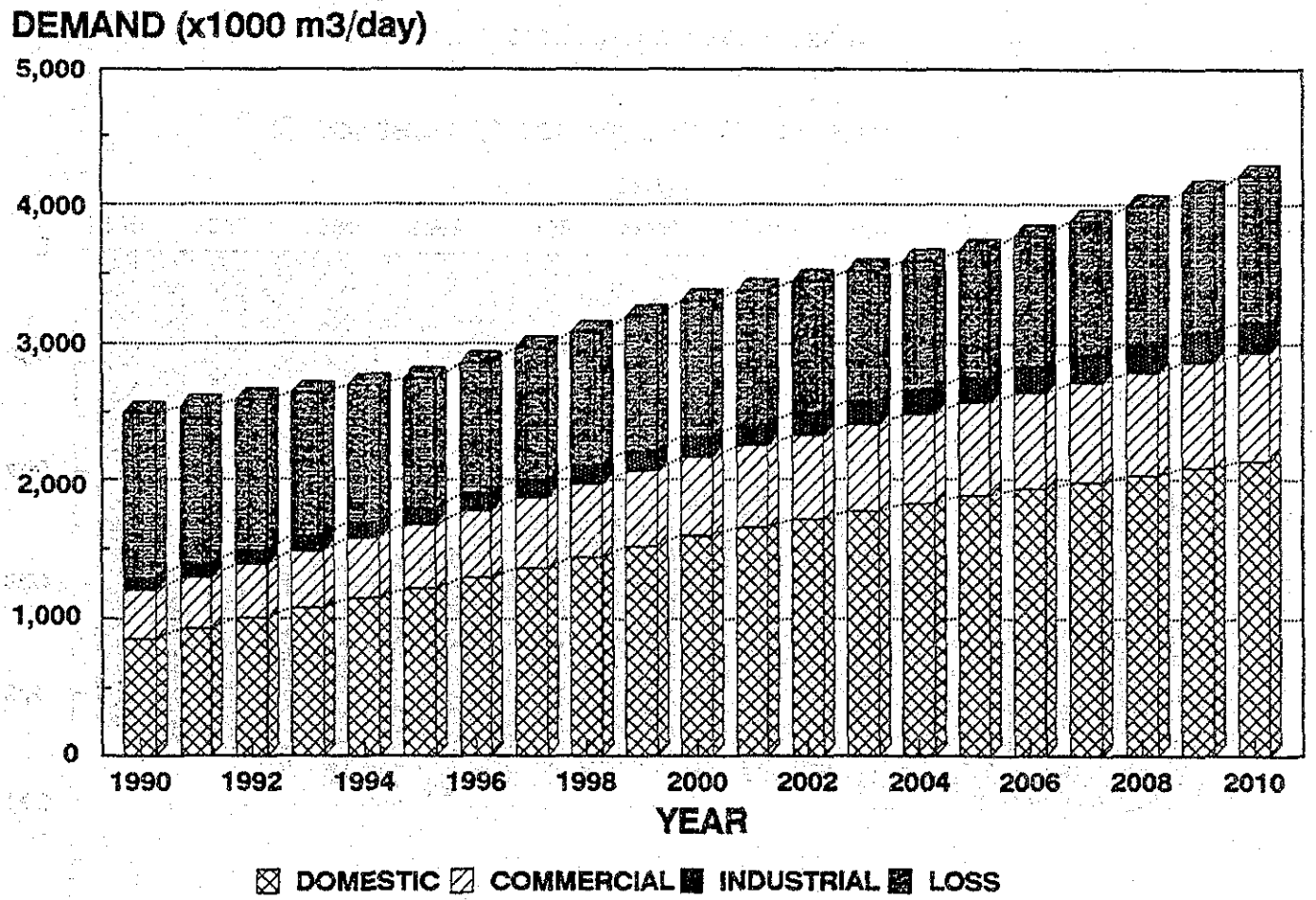

FIGURE 6.2.1 MWSS WATER DEMAND

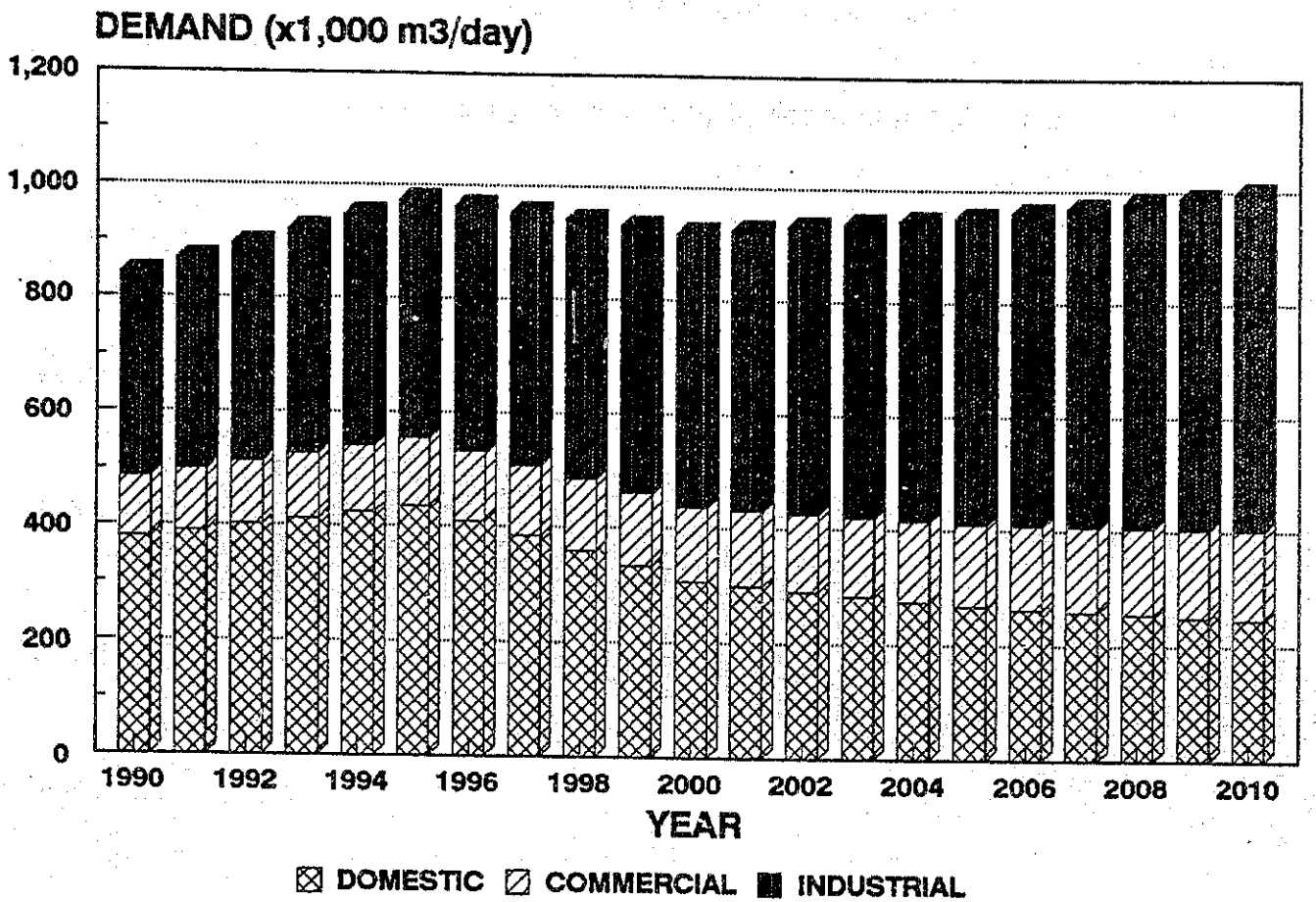

FIGURE 6.2.2 PRIVATE WATER DEMAND

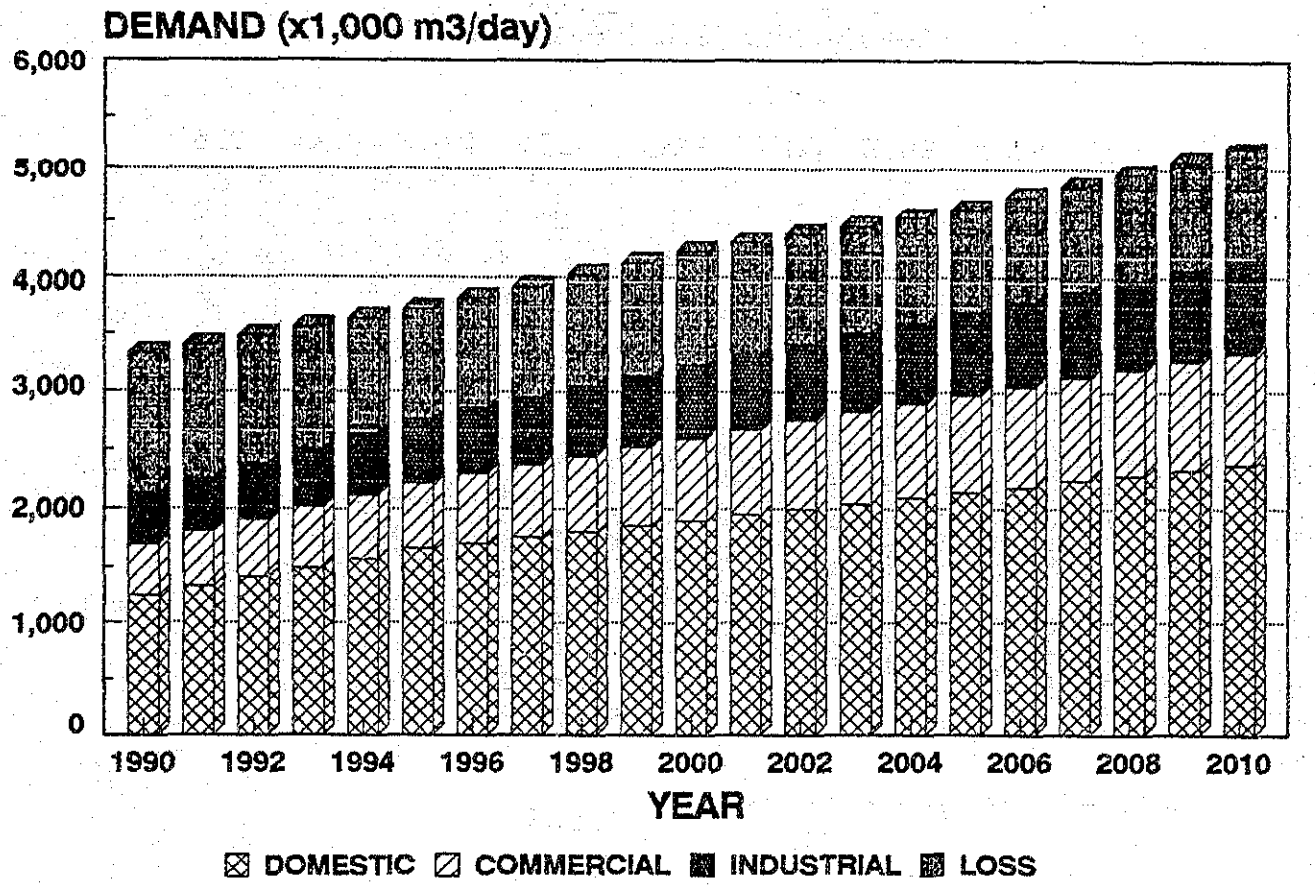

FIGURE 6.2.3 TOTAL WATER DEMAND (MWSS+PRIVATE)

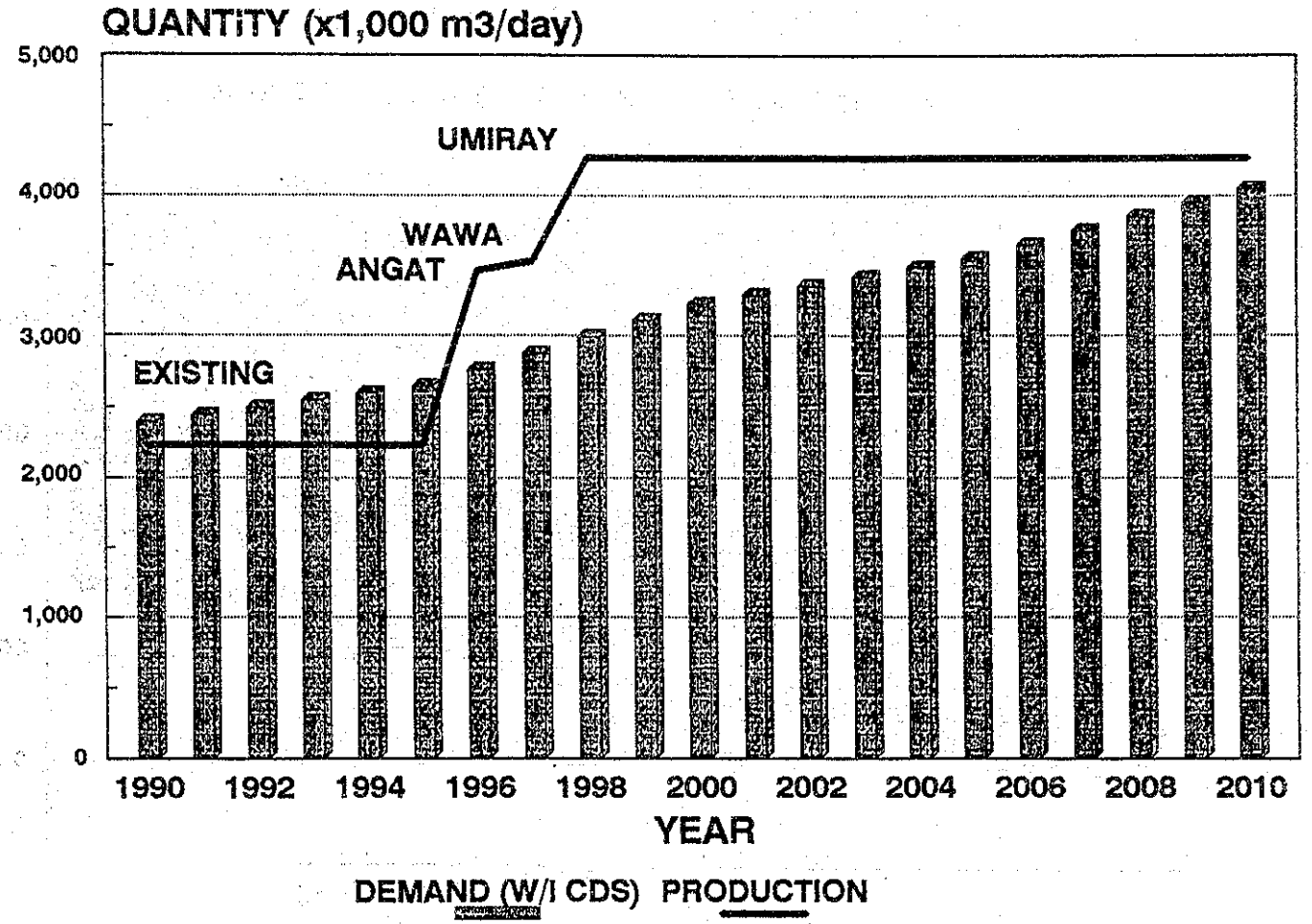

FIGURE 6.2.4 DEMAND VS. SUPPLY CAPACITY (WITHIN CDS)

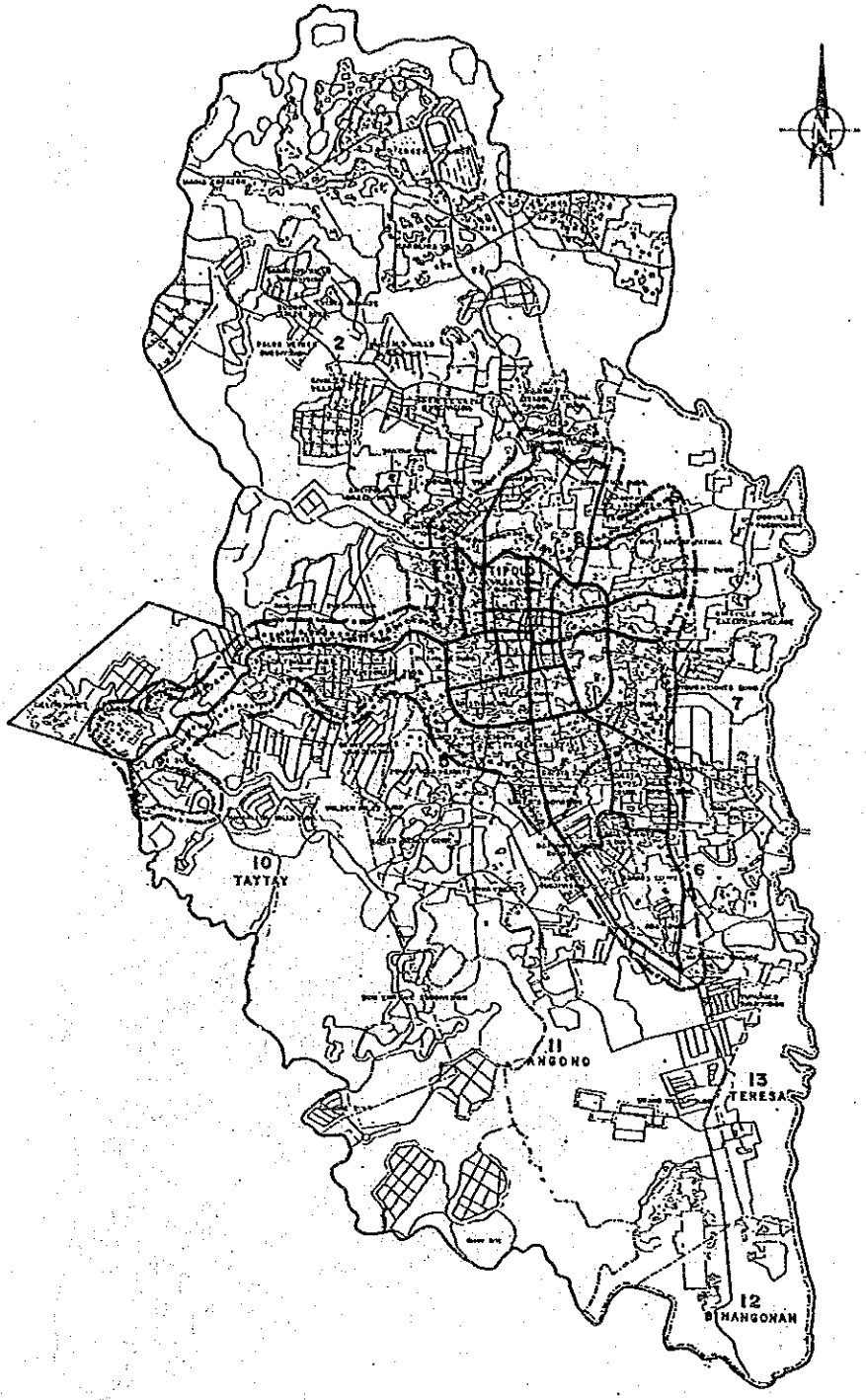

BARANGAY / MUNICIPALITY

1. Bagong Nayon
2. Sto. Cristo
3. De la Paz
4. Beverly Hills
5. San Roque
6. Dolores
7. San Jose
8. San Isidro
9. San Luis
10. Taytay
11. Angono
12. Binangonan
13. Teresa

STUDY AREA
WATER BASIN ZONE
MUNICIPALITY BOUNDARY
BARANGAY BOUNDARY

LEGEND:

PROPOSED PIPE LINE
1995 SERVICE COVERAGE
2000 SERVICE COVERAGE

STUDY FOR THE GROUNDWATER DEVELOPMENT IN METRO MANILA
JAPAN INTERNATIONAL COOPERATION AGENCY

FIGURE 6.2.5
MWSS SERVICE COVERAGE IN 1995 AND 2000

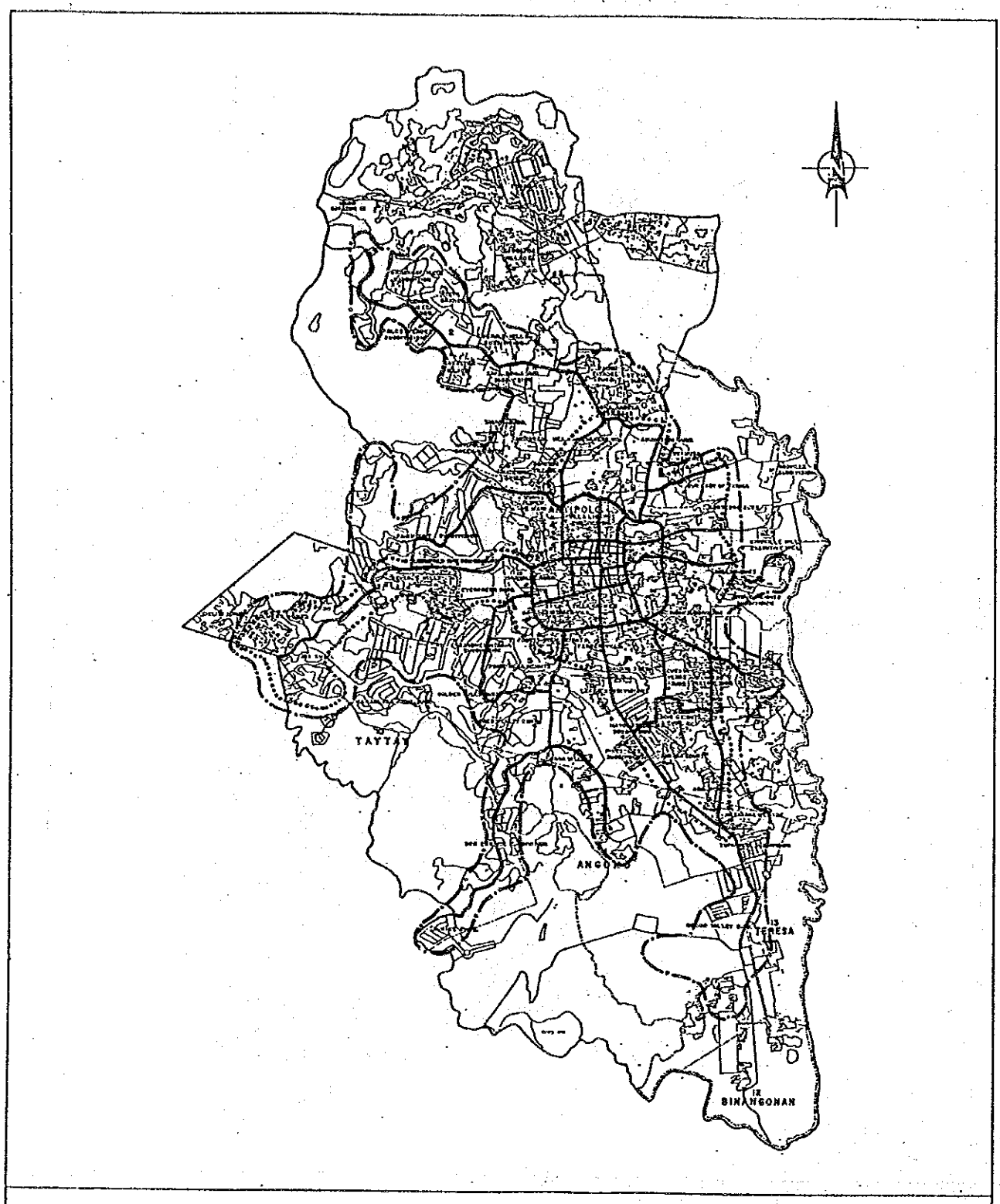

STUDY FOR THE GROUNDWATER DEVELOPMENT IN METRO MANILA

JAPAN INTERNATIONAL COOPERATION AGENCY

FIGURE 6.2.6 MWSS SERVICE COVERAGE IN 2010

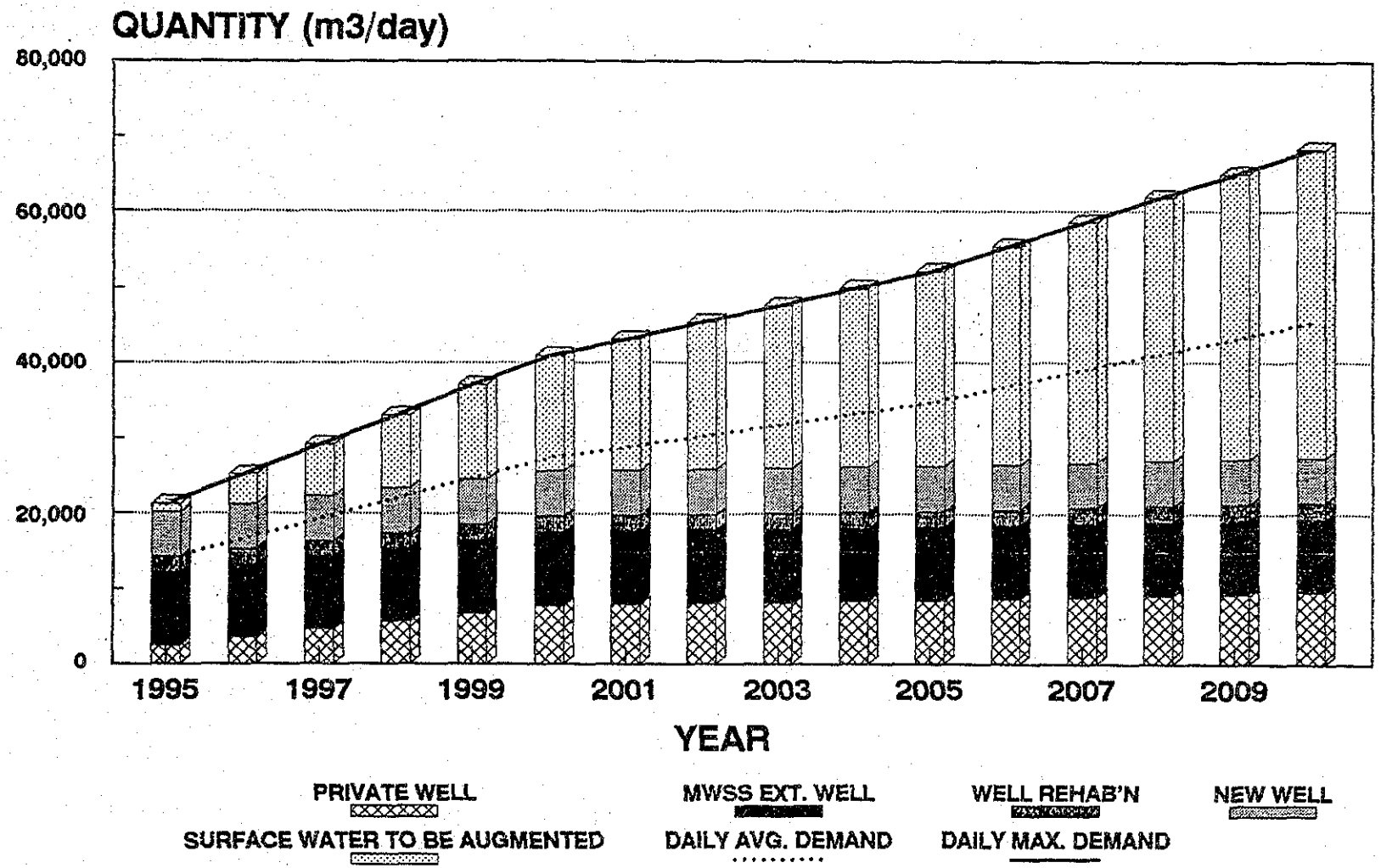

FIGURE 6.2.7 DEMAND VS. SUPPLY CAPACITY
(WITHIN MWSS SERVICE AREA IN ANTIPOLO)

CHAPTER 7

EVALUATION OF GROUNDWATER RESOURCES

CHAPTER 7 EVALUATION OF GROUNDWATER RESOURCES

CONTENTS

LIST OF TABLES

LIST OF FIGURES

CHAPTER 7 EVALUATION OF WATER RESOURCES

7.1 GROUNDWATER MODELING

7.1.1 Groundwater Flow Model

The computer model used for the study is a quasi three-dimensional groundwater flow model (Q3P model). Its basic concept is that the groundwater in the main confined aquifer is supplied by lateral flow through the aquifer and by vertical flow through the aquitard from the overlying phreatic aquifer (Figure 7.1.1.).

Q3P solves the groundwater flow equation using a finite-element approximation. The model is based on a rectangular finite-element grid. The model is applicable to two-dimensional or three-dimensional problems even in multi-aquifer systems involving steady-state or nonsteady-state flow.

The model computes changes in piezometric heads over time caused by changes in groundwater pumpage and groundwater recharge. If future plans of groundwater pumpage are inputted to the model, it can calculate future piezometric heads.

The required input data for the model are as follows:

for model framework

Element data
Node data
Boundary conditions
Model control card

for hydrogeologic settings

Transmissivity
Storage coefficient
Aquitard thickness
Aquitard permeability

Phreatic water level
Initial piezometric heads
Direct recharge data

for groundwater use

Discharge data

The output data from the model are:

Piezometric heads distribution at each time-step
Changes of piezometric heads at specified nodes
Water balance components in specified area

The model assumes that hydrogeologic parameters such as transmissivity, storage coefficient and leakance are not affected by changes in piezometric heads. Also, the model needs to assume that those parameters and boundary conditions do not change over time. The phreatic water levels are assumed to be constant over time.

The model must be calibrated before starting actual calculations. The main procedure of model calibration involves specifying the boundary conditions and the identification of some poorly reliable hydrogeologic parameters. Generally the model is verified by the comparison of calculated piezometric heads with actual piezometric heads. Figure 7.1.2. shows the general flow of model calibration.

After all parameters and boundary conditions are fixed, the model can compute future piezometric heads based on future groundwater pumpage plans and future recharge estimates.

The groundwater flow model was applied to the Antipolo groundwater basin and the Metro Manila groundwater basin (Figure 7.1.3).

7.1.2 Solute Transport Model

The two-dimensional solute transport and dispersion model (MOC model) used in the study was originally devised by L. F. Konikow and J. D. Bredehoeft in 1978.

MOC is a two-dimensional model for the simulation of non-conservative solute transport in saturated groundwater systems. It computes changes in the spatial concentration distribution over time that are caused by convective transport, hydrodynamic dispersion, mixing or dilution from recharge, and chemical reactions.

The chemical reactions include first-order irreversible rate reaction (such as radioactive decay), reversible equilibrium-controlled absorption with linear, Fruendlich or Langmuir isotherms, and reversible equilibrium-controlled ion exchange for monovalent or divalent ions.

The model assumes that fluid density variations, viscosity changes and temperature gradients do not affect the velocity distribution. MOC does allow modeling heterogeneous and/or anisotropic aquifers.

The calculation procedure of MOC model is shown in Figure 7.1.4. MOC couples the groundwater flow equation with the non-conservative solute transport equation. The computer program uses ADI or SIP procedure to solve the finite-difference approximation of the groundwater flow equation. The SIP procedure for solving the groundwater equation is most useful when areal discontinuities in transmissivity exists or when the ADI solution does not converge.

MOC uses the method of characteristics to solve the solute transport equation. It uses a particle tracking method to represent convective transport and a two-step explicit procedure to solve the finite-difference equation describing the effects of hydrodynamic dispersion, fluid sources or sinks, and divergence of velocity.

The explicit procedure is subject to stability criteria, but the program automatically determines and implements the time-step limitations necessary to satisfy the stability criteria.

MOC uses a rectangular, block-centered, finite-difference grid for flow and transport calculations. The grid size for flow calculations is limited to 40 rows and 40 columns. The grid size for transport calculations is limited to 20 rows and 20 columns which can be assigned to any area of the flow grid.

The program allows for spatially varying diffuse recharge or discharge, saturated thickness, transmissivity, boundary conditions, initial heads and initial concentrations and unlimited number of injection or withdrawal wells.

The required input data for the model are as follows:

for model framework

- Node data
- Model control card
- Transport calculation control card

for hydrogeologic settings

- Transmissivity (Txx and Tyy)
- Storage coefficient
- Aquifer thickness
- Leakance
- Initial heads
- Recharge data
- Discharge data

for transport calculation

- Maximum number of particles
- Initial number of particles per node
- Bulk density of the solid
- Langmuir adsorption coefficient
- Maximum adsorption capacity
- Half-life of the solute
- Reaction specifier
- Effective porosity
- Longitudinal and transverse dispersivity
- Source concentration
- Initial concentration

The output data from the model are:

- Summarized input data table

Heads distribution in each time step
Changes of heads and concentrations at specified nodes
Water balance components in modeled area
Concentration distribution in each time-step
Chemical mass balance
Computed velocities
Computed dispersivity

The model must be calibrated before starting actual calculations. The main procedure of model calibration involves specifying boundary conditions and the identification of some poorly reliable hydrogeologic parameters and physical/chemical parameters. Generally the model should first be verified by the comparison of calculated heads with actual heads. After fixing hydrogeologic parameters and boundary conditions, the identification for solute transport calculation of parameters, boundary conditions and initial conditions will be by comparison of their actual distribution of concentration.

After all parameters and boundary conditions are fixed, the model can then compute future heads and future concentrations based on future groundwater pumpage plans and future recharge estimates.

The solute transport model was applied to the Las Piñas area to reveal the mechanism of saltwater intrusion (Figure 7.1.3).

7.2 ANTIPOLO GROUNDWATER BASIN

7.2.1 Model Parameters and Boundary Conditions

The quasi three-dimensional groundwater model was applied to the aquifer system in Antipolo plateau, eastern part of Metro Manila (see Figure 7.1.3). The Antipolo plateau forms an independent groundwater basin at the place where the Guadalupe Formation overlies the altered spilitic basalt of the Kinabuan Formation.

Member III of the Guadalupe Formation (Gs) forms fairly good aquifers. Groundwater in the uppermost weathered beds is in the phreatic condition. Groundwater in lower part of the member III is confined and forms

a main aquifer in Antipolo plateau. Member IV (Gmd) forms an aquitard or aquifuge. The altered basaltic rocks form a hydrogeologic basement of the Antipolo groundwater basin.

The quasi three-dimensional model was used to examine the dynamic groundwater flow in the basin and the effect of groundwater development. Various hydrogeologic data and parameters required for the model had been previously prepared.

A number of simplifications had been made in the representation of the hydrogeologic system in order to analyze the dynamic behavior of groundwater flow. The confined aquifer (Gs) was modeled as a main confined aquifer which is hydraulically connected to the overlying phreatic aquifer through confining layer.

The finite-element grid used in the model is shown in Figure 7.2.1. The model domain has an area of 24.56 km^2 which was divided into 393 rectangular elements of 250m x 250m. The number of elements in the x and y coordinates are 34 and 16, respectively. The number of nodes in the domain at which the heads are computed is 448.

(1) Boundary Conditions

Two different boundary conditions were specified based on the hydrogeologic interpretations (Figure 7.2.2). The outlets of major valleys were modeled as constant-head boundaries. Also assigned as a constant-head boundary is the southern perimeter of the modeled area where the aquifer in the plateau may extend south towards Laguna de Bay. The head values of constant-head boundaries were drawn from the initial heads estimation.

The rest of the nodes along the modeled perimeter were modeled as no-flow boundaries.

(2) Model Parameters

Input parameters used in the model were those collected/measured by the Study Team during stages I to III. After data processing was completed, input data for the Q3P model were prepared. These parameters were input-

ted to the model, and then modified and identified through model calibration. The period of model calibration is ten (10) years, from 1981 to 1990.

Model parameters used in the model are as follows:

(a) Transmissivity

Because of inadequate pumping test data in the modeled area, the initial transmissivity value was modeled uniformly as 100m²/d. Throughout the steady-state calibration of the model, transmissivity values from a minimum of 10 m²/d to a maximum of 2,000m²/d were identified. High transmissivity values had to be assigned to the elements along the constant-head boundaries, rivers, and around the center part of the basin. On the other hand, low transmissivity values had to be assigned to the area where the basement rocks are exposed and/or where the topographic levels are higher.

(b) Storage coefficient

The values of storage coefficient were initially and uniformly assigned as $1x10^{-3}$ because of the lack of actual data. During the nonsteady-state calculation, the values were modified by comparison of model results with field observations of piezometric heads.

Further, the Q3P model was arranged to simulate changes of piezometric heads in 1990 using estimated three-day recharge and discharge data for the identification of storage coefficient. Throughout the 120-step simulation, done with checking of range of piezometric heads, the values of storage coefficient were finally identified as 0.1 to 0.05.

(c) Aquitard thickness and permeability

The thickness and permeability of aquitard control the leakage recharge to the confined aquifer. From a result of monitored piezometric heads, the recharge in the Antipolo basin is assumed to occur as the direct recharge. Therefore, the thickness of aquitard was uniformly modeled as 20m with its permeability as

0m/d.

(d) Phreatic water level and initial heads

The phreatic water level is an important leakage recharge parameter. The Antipolo basin model assumes the recharge to be only the direct recharge from precipitation so that dummy data were inputted to the model.

The initial piezometric heads were estimated from the steady-state simulation because no figures were available for the actual heads in 1981. For the steady-state simulation, the input initial heads were prepared based on geomorphological analyses. A river level map was made from topographic maps using the same grid to model the area. The initial heads were then assumed to be 10m below the river level.

After 30 steps (30 years) of steady-state calculation using the recharge and discharge data of 1981, the stabilized piezometric heads were noted. These were then used as the initial heads of 1981 for the nonsteady-state simulation.

(e) Direct recharge

The direct recharge was estimated from the water balance computation. The daily rainfall measured at the Boso-boso station and the Science Garden station plus the daily pan-evaporation measured at Science garden were used to estimate direct recharge. The pan-evaporation data were used to compute the actual soil evaporation and evapotranspiration. The soil characteristics viz. soil type, moisture holding capacity and thickness of soil zone, as well as vegetation characteristics were taken into account in determining the surplus water from the soil zone.

Figure 7.2.3 shows the annual rainfall and computed recharge at Boso-boso station from 1981 to 1990. The annual recharge values were inputted to the model. Figure 7.2.4 shows the water balance components in the Antipolo basin using Science Garden's data from 1962 to 1989.

7.2.2 Verification of the Model

Model verification is carried out to identify input parameters and assigned boundary conditions. This process is the most important and most complicated work in groundwater modeling because the areal quantification of various parameters, which play significant roles in the groundwater regime, should be done under actual hydrogeologic constraints. Thus, the verification of the model yields a better insight on dynamic groundwater behavior in the area as well as on the limitations of the model.

(1) Steady-state Simulation

The calibration of the model was initially carried out in steady-state conditions to identify the initial heads and transmissivity of the model. The simulated piezometric heads were observed at the selected points shown in Figure 7.2.5. Using constant, year-1981 pumping rate throughout the 30-year period (30 time-steps), computation of groundwater heads proceeded on a trial-and-error basis until it reached the point when the drops in head had become approximately zero (Figure 7.2.6).

Throughout the steady-state simulation, transmissivity and boundary conditions were modified. The piezometric heads obtained from the 30-year steady-state calculation were extrapolated and used as the initial groundwater heads in 1981 for nonsteady-state simulation (Figure 7.2.7). Figure 7.2.8 shows the difference between initial piezometric heads and elevations of the bottom of the aquifer. The initial piezometric heads are located at more than 100m above the bottom of aquifer around the central part of the basin.

(2) Nonsteady-state Simulation

The nonsteady-state simulation from 1981 to 1990 was carried out to simulate transient groundwater flow and decline of piezometric heads due to groundwater pumpage. The storage coefficient was also modified and identified throughout the simulation. The simulation period is divided into 10 time-steps, each time-step having a duration of 1 year (365 days).

The groundwater discharge data in the modeled area were prepared from the groundwater use survey of the Study Team. There are ten (10) MWSS wells and twenty six (26) private wells in the area. Figure 7.2.9 shows the annual groundwater production from 1981 to 1990 based on the monthly production reports of MWSS wells and field investigations of private wells. The total groundwater production has increased from 11,419 CMD in 1981 to 19,456 CMD in 1990. The year-wise distribution of the discharge data from 1981 to 1990 were arranged for computer simulation. Figures 7.2.10 and 7.2.11 show the groundwater pumpage in 1981 and 1990, respectively.

Throughout the nonsteady-state simulation, the storage coefficient was modified through comparison of computed heads with actual heads. Further, the Q3P model was arranged to simulate changes of piezometric heads in 1990 using estimated 3-day recharge and discharge data for the identification of storage coefficient. The final storage coefficient ranges from 0.05 to 0.1.

Figure 7.2.12 shows the simulated piezometric contours in 1990. The difference between the simulated heads and bottom elevations of the aquifer is shown in Figure 7.2.13. The piezometric heads since 1981 have declined at a maximum depth of 16.4m due to the increase of discharge (Figure 7.2.14).

7.2.3 Optimal Pumpage

(1) Future Pumpage Plans

The Antipolo groundwater flow model simulated future piezometric heads for the design of optimal pumpage in the area. The simulated future period is up to the year 2010. Thus piezometric heads of 30 time-steps (30 years) from 1981 to 2010 were simulated continuously. Three (3) cases were prepared for future simulation based on the well design of new MWSS wells and the rehabilitation plan. These are:

(a) The discharge of MWSS wells in 1990 will continue up to 2010.
(b) New MWSS wells will be constructed and will pump from year 1991 to 2010 at a rate of 830 CMD per well. The discharge of existing MWSS wells will not change.

(c) New MWSS wells will be constructed and will pump from 1991 to 2010 at the rate of 830 CMD per well. The discharge of existing MWSS wells will be augmented 207 CMD per well from 1991 by well rehabilitation.

It is assumed in the above cases that the discharge of existing private wells will be the same as that in 1990 and no new private wells will be constructed. It is also assumed that future recharge will be uniform from 1991 to 2010.

(2) Future Recharge Evaluation

The recharge from rainfall is the most important parameter for evaluating the future groundwater potential in the area. As mentioned before, a 10-year recharge estimation had been carried out using daily rainfall and daily pan-evaporation data. The estimated recharge took a wide range--from 337.9mm/year to 1310.8mm/year, depending on the amount of precipitation and rainfall pattern.

The long-term statistical analysis of rainfall and recharge aids the evaluation of groundwater recharge. The meteorological data at the Sumulong and Antipolo stations were used for the analysis. The 62-year data from 1911 to 1972 were collected and arranged for annual recharge estimation. The annual rainfall and estimated annual recharge are shown in Figure 7.2.15. The average, minimum and maximum recharge for the 26-year period are 636.0mm/year, 223.3mm/year, 1682.6mm/year, respectively.

A probability analysis using the Thomas method was done. The results are shown in Table 7.2.1.

Table 7.2.1 RESULTS OF DROUGHT PROBABILITY ANALYSIS OF RECHARGE (26-YEAR DATA OF SCIENCE GARDEN)

Drought Probability	Recharge (mm/year)	Recharge to the Basin (CMD)
(Simple average)	636.0	42,799
2 years	589.9	39,697
3 years	495.1	33,318
5 years	418.8	28,183
10 years	350.2	23,567
20 years	302.0	20,323

For the future simulation, the recharge value for a 5-year drought probability was employed on the safe side. The recharge value of 28,183 CMD is the maximum groundwater potential from the water balance point of view.

(3) Future Simulation

(a) Case (a)

The evaluated recharge and the discharge in 1990 were inputted to the model. Figure 7.2.16 shows that the simulated piezometric heads will decline even though the discharge is the same as that for 1990. The simulated piezometric contours and the heights from the aquifer bottom are shown in Figure 7.2.17 and 7.2.18, respectively. The maximum drawdown from 1991 to 2010 is expected as 52.4m.

(b) Case (b)

The exploitable groundwater potential, possible number and locations of new MWSS wells were examined under different recharge conditions. The discharge of existing MWSS wells and existing private wells in 1990 will continue up to 2010. The following are the criteria for locating new wells:

i) New wells should be located where the simulated piezometric heights of Case (a) in year 2010 (Figure 7.2.18) are more than 30m because the drawdown of new wells are estimated to be 20m to 21m from static level.

ii) Existing pumping grids should be avoided for the new wells' location.

iii) The total discharge of existing wells and new wells should not exceed the recharge to the basin.

iv) Simulated piezometric heights up to the year 2010 using the new discharge data involve the new wells' discharge. The simulated piezometric heights at the sites of new wells should be more than 21m.

The possible number and locations of new wells were identified under several discharge conditions and are given in Table 7.2.1. Evaluation results are given in Table 7.2.2.

Table 7.2.2 AVAILABLE NUMBER OF NEW WELLS AND EXPLOITABLE DISCHARGE UNDER DIFFERENT RECHARGE CONDITIONS

Drought Probability	Recharge (CMD)	Total Discharge (CMD)	Available New Wells (Nos.)	Exploitable Discharge (CMD)
2 years	39,697	36,056	20	16,660
3 years	33,318	30,246	13	10,790
5 years	28,183	27,756	10	8,300
10 years	23,567	22,776	4	3,320
20 years	20,323	20,286	1	830

In this case, the construction of ten (10) new wells may be optimal for future groundwater development in the area.

(c) Case (c)

A plan for the construction of new wells, as well as the augmentation of existing MWSS wells by well rehabilitation, are examined in this case. The discharge of each existing MWSS well will be augmented by 207 CMD. So, the total augmentation of existing MWSS wells is:

207 CMD x (10 MWSS existing wells) = 2,070 CMD

Under the recharge conditions of a 5-year drought probability, the total recharge to the basin is estimated as 28,183 CMD. The existing wells were pumping 19,456 CMD in 1990; so, the maximum available water from the new wells is:

28,183 CMD - 19,456 CMD - 2,070 CMD = 6,657 CMD

The simulation study that was carried out to make an optimal plan of groundwater development in the area had the piezometric heads in 2010 computed first using the increased discharge of existing wells. The number and location of new wells were determined using the same criteria as Case (b).

As a result, seven (7) new MWSS wells were found to satisfy the criteria. The optimal distribution of future discharge is shown in Figure 7.2.19. Figure 7.2.20 and Figure 7.2.21 show the piezometric contours and piezometric heights from aquifer bottom in 2010, respectively. The piezometric heads will be lower than 100m at the central part of the basin, but the piezometric heights at the new sites will be more than 21m. Figure 7.2.22 shows that the piezometric heads will almost be stabilized by the year 2010.

The total discharge in the basin is:

19,456 CMD +2,070 CMD +5,810 CMD (7 new wells) = 27,334 CMD

Figure 7.2.23 shows the estimated discharge and recharge in the optimal plan.

(4) Optimal Plan for Groundwater Development

Under the conditions mentioned above, the optimal groundwater development plan in Antipolo basin is summarized as follows:

i) Rehabilitate existing ten (10) MWSS wells
ii) Construct seven (7) new MWSS wells

However, it should be noted that this optimal plan was made under various assumptions, the most important and problematic of which is the remaining constant of the future pumpage of private wells. Actually there are many unknown factors to consider in predicting future pumpage of privately-owned wells. These may be correlated with population growth, but still many assumptions are needed.

The optimal plan was carefully examined from the water balance and hydrogeologic conditions in the basin. The groundwater potential also was evaluated on the safe side.

From the maximum groundwater potential of 29,287 CMD, existing wells are already pumping 19,456 CMD. So the maximum available water in the future is estimated only as 10,000 CMD.

Some problems could occur during the lowering of piezometric heads as reactions to groundwater development. One of these problems is the decreasing yield of existing wells. Some of these wells are so shallow that they may not be able to yield water at the same present rate. Some wells may have to install higher capacity pumps.

Since the groundwater potential and source of groundwater recharge are limited in the area, a countermeasure for groundwater conservation should also be taken into account for better utilization of groundwater resources.

7.3 METRO MANILA GROUNDWATER BASIN

The quasi three-dimensional groundwater flow model (Q3P model) was applied to the aquifer system in the Metro Manila groundwater basin.

The Guadalupe formation and Alluvium comprise a complex and confined aquifer system in the Metro Manila groundwater basin.

The eastern margin of the basin is bounded by a hilly area consisting of Pre-Quaternary formations. The aquifer system continues across northern and southern boundaries. The western margin and southeastern are bounded by Manila Bay and Laguna de Bay, respectively.

The hydrogeologic basement in the basin consists of Pre-Quaternary formations, but detailed information on basement rocks have not been collected because these are overlain by the thick Guadalupe formation. The thickness of Guadalupe aquifer system may be more than 1,000m in Manila Bay, but detailed structures about the basement of Guadalupe formation have yet to be known.

Conceptualizations and quantifications have been made in the representation of the groundwater regime in order to analyze the dynamic behavior of groundwater flow. The aquifer system up to a depth of 300m was modeled as a main confined aquifer because most of the wells in the area extract groundwater at a depth of 300m. The main aquifer is hydraulically connected to the overlying phreatic aquifer through a confining layer.

The finite-element grid used in the model is shown in Figure 7.3.1. The model domain has an area of 1404.7km^2 and is divided into 754 rectangular elements of 1350m x 1380m, which correspond to 45 seconds of longitude and latitude. The number of elements in the x and y coordinates are 28 and 35, respectively. The number of nodes in the domain where the heads are computed is 829.

7.3.1 Model Parameters and Boundary Conditions

(1) Boundary Conditions

Three (3) different boundary conditions were specified based on the hydrogeologic interpretations (Figure 7.3.10). The boundary of the eastern margin of the basin was treated as a no-flow boundary. The northern and southern perimeters of the modeled area where the aquifer extends out were assigned as constant-flow boundaries. Constant-head

boundaries were assigned to Manila bay and Laguna de Bay at the place where the distance from coastlines is about 5km. The area between constant-head boundaries and actual coastlines was regarded as cushion zone.

(2) Model Parameters

Input parameters used in the model were those collected/measured by the Study Team during Stage I to III. After data processing was completed, input data for the Q3P model were prepared. These parameters were inputted to the model, and then modified and identified through model calibration. The period of model calibration is the ten (10) years from 1981 to 1990.

Model parameters used in the model are as follows.

(a) Transmissivity

Transmissivity was estimated from the data on specific capacity of existing wells and the pumping tests results compiled by the Study Team. The methodology of the estimation is as mentioned in Chapter 3. Transmissivity values range from $10m^2/d$ to $315m^2/d$.

(b) Storage coefficient

The initial values of storage coefficient were uniformly assigned as $1x10^{-3}$ because of the lack of actual data. But during the steady-state and nonsteady-state calculations, the values were modified by comparison of model results with field observations of piezometric heads. Finally, $1x10^{-3}$ to $1x10^{4}$ of storage coefficient is assigned to the model.

(c) Aquitard thickness and permeability

The thickness (b') and permeability of aquitard (k') control the leakage recharge to the confined aquifer as leakance (k'/b'). The aquitard thickness was obtained from the clay content map which was prepared from the well columnar sections collected by the Study Team. The thickness ranges from 7m to 53m.

The permeability of aquitard is one of the unknown parameters in the area. Thus, initial values of the permeability were uniformly assigned as $1x10^{-3}$m/d, and then modified and identified throughout the model calibrations. Final permeability ranges from $1x10^{-1}$m/d to $1x10^{-9}$m/d. The computed leakance values vary from $1x10^{-6}$/d to $2x10^{-3}$/d.

(d) Phreatic water level and initial heads

The phreatic water level is an important leakage recharge parameter. This was estimated from a geomorphological analyses. A river level map was made from topographic maps using the same grid to model the area. The phreatic water level was then assumed to be 10m below the river level. The model assumes that the phreatic water levels are invariant during the simulation.

The initial piezometric heads for the steady-state simulation were estimated using the same method mentioned. The initial piezometric heads in 1981 for the nonsteady-state simulation were prepared from the data of MWSP II (1983).

(e) Direct recharge

The direct recharge area was demarcated based on the results of groundwater leveling mentioned in Chapter 3.5.1. The model assumes that leakage recharge does not occur at the direct recharge area.

The values of direct recharge were obtained from the water balance study mentioned in Chapter 3.6. The input average recharge is 183.1mm/year, or about 8% of annual rainfall.

7.3.2 Verification of the Model

(1) Steady-state Simulation

Model verification is carried out to identify input parameters and assigned boundary conditions. This process is the most important and most complicated work in groundwater modeling because areal quantification of various parameters, which play significant roles in the ground-

water regime, should be done under actual hydrogeologic constraints. Thus, the verification of the model yields a better insight on dynamic groundwater behavior in the area as well as on the limitations of the model.

The calibration of the model was initially carried out in steady-state conditions to identify initial heads, storage coefficient, leakance and boundary conditions of the model. The simulated piezometric heads were observed at the selected points shown in Figure 7.3.3. Using a constant, year-1981 pumping rate (see Figure 7.3.4) throughout the 30-year period (30 time-steps), computation of groundwater heads proceeded on a trial and error basis until it reached the point when the difference between the computed and actual heads in 1981 had become approximately zero. Figure 7.3.5 shows the changes of piezometric heads at observation points during the steady-state simulation. The simulated piezometric contours after the 30-year steady-state calculation are shown in Figure 7.3.6.

(2) Nonsteady-state Simulation

The nonsteady-state simulation from 1981 to 1990 was carried out to simulate transient groundwater flow and decline of piezometric heads due to groundwater pumpage. The actual piezometric heads measured in 1981 were used as initial heads in the model. The leakance and storage coefficient were modified and identified throughout the simulation. The simulation period is divided into 10 time-steps, each time-step having 1 year (365 days).

The groundwater discharge data in the modeled area were prepared from the groundwater use survey of the Study Team. Figure 7.3.7 shows the annual groundwater production from 1981 to 1990 in the modeled area. Total groundwater production decreased from 333.1 MCM/year in 1981 to 310.5 MCM/year in 1990, but the production of MWSS wells increased from 18.2 MCM/year in 1981 to 29.0 MCM/year in 1990. The discharge data were arranged for computer simulation. Figure 7.3.8 shows the discharge distribution in 1990.

Throughout the nonsteady-state simulation, leakance (permeability of aquitard) and storage coefficient were modified and identified by com-

parison of computed heads with actual heads. The leakance is the most sensitive parameter in the model so that more than hundred times of test simulation was carried out to determine this parameter.

Figure 7.3.9 shows the simulated piezometric contours in 1990. The changes of piezometric heads at the observation points are shown in Figure 7.3.10. Recovery of the piezometric heads in the northern part to the central part of Metro Manila (Caloocan, Valenzuela, Manila, the western part of Quezon city, San Juan, Mandaluyong and western part of Pasig) and the Cavite area is reasonably simulated due to decreases of the discharge. However, the piezometric heads in the southern part of Metro Manila (Taguig, Parañaque, Muntinlupa, Las Piñas, Bacoor, Imus, kawit, Noveleta and Rosario) went down because the discharge increased in those areas.

7.3.3 Prediction of Future Groundwater Levels

The model can simulate future piezometric heads using future recharge and discharge plans. The duration of future simulation is the 20 years from 1991 up to 2010. The future piezometric heads are computed based on the simulated piezometric heads of 1990. The model thus computed piezometric heads at 30 time-steps (the 30 years from 1981 to 2010).

The evaluation of the future recharge to the basin is contained in the water balance study in Chapter 3.6. Five (5) cases of future groundwater levels were prepared based on future water demand projections. The scenarios used in projecting future demand were also adopted for these cases.

(a) Discharge in 1990 continues up to 2010.
(b) Scenario 1
(c) Scenario 2
(d) Scenario 3
(e) Scenario 4

Table 7.3.1 SUMMARIZES THE CHARACTERISTIC THOSE FOUR SCENARIOS.

Table 7.3.1 CHARACTERISTICS OF THE SCENARIOS

Scenario No.	MWSS Surface Water Supply Projects	Future Pumpage of Commercial & Industrial Private Wells	CDS Connection in Cavite MSA
1	On-schedule completion of ongoing projects	Increasing (1	Bacoor 100% covered, Kawit 50%, others 0%
2	Same as Scenario 1	Increases (2 up to year-2000, thereafter pumpage is constant	All municipalities covered
3	Same as Scenario 1	Increases (2 up to year-1995, thereafter pumpage is constant	All municipalities covered
4	Two years delay of completion of ongoing projects	Same as Scenario 1	Same as Scenario 1

Note: (1 With respect to future demand increases but maintaining year-1990 percentage shares
(2 With respect to future demand increases and up to the year indicated

Yearly groundwater production of each scenario in the modeled area is shown in Figure 7.3.11. In each graph, groundwater production from 1981 until 1990 is actual figure. The discharge distribution maps in the year 2010 of Scenario 1 and 2 are shown in Figure 7.3.12. The discharge distribution of Scenario 3 and 4 are shown in Figure 7.3.13.

The results of simulation are as follows:

(a) Discharge in 1990 continues up to 2010

This case assumes that the discharge of 316.572 MCM in 1990 continues up to 2010. As shown in Figure 7.3.14, and in comparison with heads in 1990, the piezometric heads in 2010 will recover at a maximum of 10.7m in the central part of Metro Manila. Decline of heads can be seen in the northern part, eastern part (along Marikina river), and southern to southwestern part of Metro Manila. A maximum drawdown of 21.7m is predicted at the northern part of Quezon City. A 16.9m drawdown will occur in Rosario.

(b) Scenario 1

The simulated piezometric contours in 2010 (Figure 7.3.14 (a)) show that a large piezometric depression appears in northwestern Metro Manila. The deepest portion will be lower than -170 masl. Also, considerable lowering of piezometric heads can be seen in the southwestern part, the southern and eastern parts of Metro Manila. In Cavite, the piezometric heads will be as deep as -90 masl.

The piezometric changes from 1991 to 2010 are shown in Figure 7.3.16 (a). Piezometric heads in 2010 rise in the southern part of Quezon City, Parañaque, Las Piñas and Bacoor. A maximum rise 20m of piezometric heads is predicted at the coastal area in Las Piñas because of decrement of discharge. However, heads will go down in the northern and southwestern parts of Metro Manila. Significant drawdowns such as 83m at north Valenzuela, 57m in Cavite and 37m in Pasig are predicted.

Figure 7.3.18 (a) shows that the piezometric heads in Cavite and Caloocan City declined for the period 1991 to 2000, then stabilized after. Constant decline can be seen in Pasig from 1991 to 2010. Piezometric heads in Las Piñas rose in the period from 1991 to 2000, but they go down gradually after 2005.

(c) Scenario 2

A large piezometric depression can be seen in the northwestern

part of Metro Manila (Figure 7.3.14 (b)). The lowest head will be -149 masl at north Valenzuela. A piezometric lowering belt in which the heads range from -60 to -80 masl lies from Cavite to Marikina through Muntinlupa and Parañaque.

Piezometric heads will go down 59m at north Valenzuela and 33m in Cavite since 1991 (see Figure 7.3.16 (b)). Heads will decline in most of Metro Manila from 1991 to 2000, then stabilize or slightly recover after 2001 as shown in Figure 7.3.18 (b).

(d) Scenario 3

This scenario is the most ideal case. All ongoing projects will be completed on schedule and be able to supply surface water to the area. But the simulated piezometric contours still show a large depression as deep as -134 masl in northwestern part of Metro Manila (Figure 7.3.15 (a)).

Heads in 2010 are 50m lower at north Valenzuela and 29m lower in Cavite than those in 1990 (Figure 7.3.27 (a)). Recovery of heads will occur in almost all areas from 2001 to 2005 due to decreasing discharge (Figure 7.3.18 (c)).

(e) Scenario 4

This is the scenario in which groundwater discharge is the maximum among the five cases. The discharge increases from 1991 to 2000 and from 2005 to 2010. As a result, the simulated piezometric heads (Figure 7.3.15 (b)) will be lower than those of Scenario 1.

The drawdowns of piezometric heads are estimated as 90m at north Valenzuela and 56m in Cavite (Figure 7.3.17 (b)). Piezometric heads in most of Metro Manila show significant declines until after 2000 when they decline gradually or stabilize (Figure 7.3.18 (d)).

The results of simulation show that a maximum drawdown of 50m will occur even in the case of Scenario 3 where the discharge is the smallest among the future groundwater use plans. This could cause severe saline water

intrusion and may damage even inland areas.

7.4 SALINE WATER INTRUSION MODEL

The Las Piñas area is one of those Metro Manila areas most affected by saline water intrusion. The intrusion may have been caused by the decline of the groundwater head which resulted from the increase in groundwater pumpage. The source of saline water in Las Piñas maybe seawater, but the mechanism has yet to be clarified.

Generally, in coastal areas like Las Piñas, salt water occurs underground, not at sea level but at a depth below sea level of about 40 times the height of the fresh water above sea level. This phenomenon, which is generally referred to as the Ghyben-Herzberg relation, is attributed to a hydrostatic equilibrium existing between the two fluids of different densities. But in many areas with extensive groundwater development, the Las Piñas area included, a hydrodynamic equilibrium may exist due to the dynamic groundwater flow caused by groundwater extraction so that the Ghyben-Herzberg relation cannot be applied directly.

Most researchers have approached the seawater intrusion problem by describing the landward movement of a discrete interface between seawater and freshwater. This approach assumes that seawater infiltrates solely from an offshore outcrop of the aquifer. If, however, a coastal aquifer is overlain by a leaky confining layer, this assumption is often inappropriate because seawater can potentially migrate from above. A discrete interface approach does not consider such leakage.

Therefore, applying this approach to the Las Piñas area poses some difficulties: (1) the aquifer system is divided into a shallow aquifer and deeper aquifers by leaky confining layers; (2) both the confined aquifers and the confining layers tilt toward the sea; and (3) the groundwater flow is very much disturbed by groundwater pumping so that the pattern of saltwater intrusion is different from that of the Ghyben-Herzberg relation.

According to the measurement of electric conductivity (EC) logging and water quality analysis in the Las Piñas area, saline water occurs in a

shallow aquifer up to a depth of 100m below mean sea level. In contrast, EC values and chloride concentration in deeper aquifers decrease with depth. This phenomenon may occur because seawater and saline surface water are forced to infiltrate into the underground with the lowering of piezometric head by the groundwater extraction.

The two-dimensional solute transport and dispersion model were employed to verify this hypothesis and to understand the mechanism of saline water intrusion. This model may also aid in predicting the quantity and location of saltwater resulting from future groundwater utilization or regulation.

The solute transport model was originally developed for plane two-dimensional problems, but it has been modified for vertical two-dimensional multiple aquifers system to allow for more detailed analysis of results.

A vertical two-dimensional model was made along the geological section line shown in Figure 7.4.1. This section line is almost perpendicular to the coastal line. The line which is taken as the x-axis for the model is divided into 40 nodes. Each nodal spacing is 100m and the width of 100m for each side of the line is taken into account for model domain.

Figure 7.4.2 shows the grid of the vertical two-dimensional model. Vertically, the elevations from +30m to -330m are modeled. Each cell is 15m-thick so that the volume of each cell is 15m x 100m x 200m = 300,000m^3.

The computer program of the solute-transport model allows a grid to have up to 40 rows and 40 columns for groundwater flow calculations. Because the numerical procedure requires that the outer rows and columns represent no-flow boundaries, the aquifer itself is then limited to have a maximum of 38 rows and 38 columns. Further, the grid size for transport calculation is limited to 20 rows and 20 columns which can be assigned to any area of the flow grid.

Therefore, the grid size for the flow calculation in Las Piñas is fixed as 24 rows and 40 columns, and transport subgrid size as 20 rows and 20

columns (see Figure 7.4.2).

Hydrogeologic unit of each cell viz. Alluvial clay, aquifer (sand) and aquiclude (clay) have been specified (Figure 7.4.3) based on the hydrogeologic section given in Figure 3.2.20.

7.4.1 Model Parameters and Boundary Conditions

(1) Model Parameters

Input parameters used in the model were those collected/measured by the Study Team during Stage I to III. After data processing was completed, input data for the MOC model were prepared. These parameters were inputted to the model, then modified and identified through model calibration.

Model parameters used in the model are as follows.

(a) Transmissivity

Transmissivity values of the aquifer came from the results of the pumping tests conducted in the test wells by the Study Team. Transmissivity of aquiclude was estimated from the core observation.

Table 7.4.1 summarizes the aquifer parameters of the hydrogeologic units. The apparent transmissivity (Taxx) which is inputted in the model is computed as Kxx x 200m because the width of each cell is 200m. The ratio of longitudinal transmissivity (Tyy) to transverse transmissivity (Txx) is assumed as 0.1 because the aquifer systems may be anisotropic due to the sedimental structure.

Table 7.4.1 HYDROGEOLOGIC UNITS AND AQUIFER PARAMETERS

Hydrogeologic unit (label)	Actual transmissivity Txx(m^2/d)	Permeability Kxx(m/d)	Apparent transmissivity Taxx (ft^2/s)
Alluvium (A)	(4.4)	1.46×10^{-1}	3.6×10^{-3}
Aquifer-1 (B)	220.0	7.30	181.9×10^{-3}
Aquiclude-1(C)	(4.4)	1.46×10^{-1}	3.6×10^{-3}
Aquifer-2 (D)	61.2	2.04	50.8×10^{-3}
Aquiclude-2(E)	(2.4)	8.00×10^{-2}	2.0×10^{-3}
Aquifer-3 (F)	33.6	1.12	27.9×10^{-3}
Aquiclude-3(G)	(2.4)	8.00×10^{-2}	2.0×10^{-3}
Aquifer-4 (H)	(30.0)	1.00	24.9×10^{-3}

( ): estimated values

(b) Storage coefficient

Storage coefficient was uniformly set to zero for the steady-state simulation.

(c) Aquifer thickness

Apparent thickness of aquifer for the model was uniformly set to 200m (656.2ft) in the modeled domain because the width of each cell is modeled as 200m. The actual aquifer thickness is the total thickness of the aquifer cells.

(d) Leakance

In this model constant-head boundaries were simulated by adjusting the leakance. A sufficiently high value (such as 1.0/s) was assigned at constant-head boundaries. In the rest of the area leakance was modeled as 0. The actual leakance in the aquifer system was expressed as (permeability of aquiclude)/(thickness of aquiclude).

(e) Initial heads

The initial heads were set at 0m except the uppermost cells representing the ground surface, the sea and marine pond. The water levels in the uppermost cells were treated as constant. Phreatic water levels were estimated from the topography.

(f) Direct recharge

The groundwater recharge was estimated from the water balance study. Because the actual area of each cell is 200m x 100m = 20,000m^2 the input recharge values was computed as

Input recharge at each cell (m^3)
= 20,000m^2 x estimated recharge (m^3/m^2)

The obtained recharge values were given to the uppermost cells representing ground surface.

(g) Discharge

The groundwater discharge was estimated from the results of the groundwater use survey. The location of pumping wells within the model domain were projected on the vertical grid. If the well structure was known, the depth of the well and the screen positions were also projected; otherwise, they were assumed. The discharge values were distributed into the cells where the screens are located (see Figure 7.4.2). It is assumed that if a cell expresses an aquiclude, groundwater is not extracted from the cell.

(h) Initial chloride concentration

The initial chloride concentration of the domain was set at 0mg/l except the cells representing the sea and marine ponds. The chloride concentration of seawater and marine ponds water was assumed at 21,500mg/l.

(i) Transport parameters

Several parameters were assigned for transport simulation. Table 7.4.2 summarizes inputted transport parameters.

Table 7.4.2 TRANSPORT PARAMETERS

Maximum number of particles	6400
Initial number of particles per node	9
Reaction specifier	NO REACTION
Effective porosity	0.05
Longitudinal dispersivity	7.00ft
Ratio of transverse to longitudinal dispersivity	1.0
Source concentration	21500mg/l

(2) Boundary Conditions

As shown in Figure 7.4.2, outer flows and columns of the flow grid were treated as no-flow boundaries. It was assumed that the phreatic water levels in the uppermost cells are constant so that the constant-head boundary condition was assigned to these cells. Cells which are located in the sea, rivers and marine ponds were also treated as constant-head boundaries.

7.4.2 Steady-State Simulation

Steady-state simulation was carried out for identification of the model. Duration of the simulation is 10 years, with values of input discharge and recharge being obtained from year-1990 data. The calculated piezometric heads show good agreement with the observed values without modification of hydrogeologic parameters (Figure 7.4.4).

After computing the groundwater flow, the solute transport model was calibrated. The boundary conditions of initial chloride concentration, effective porosity, longitudinal and transverse dispersivity are modified during model calibration. Figure 7.4.5 shows chloride concentration after a 10-year simulation using finalized parameters and boundary

conditions.

During model verification, several sets of parameters were prepared and inputted into the model in order to compare the saline water movement. The location of the source, and dispersivity were changed for this purpose.

(1) Saline Water Movement versus Time

The movement of saline water was studied under steady-state conditions. Figure 7.4.6 shows the steady-state piezometric contours in the flow grid and solute transport grid. Changes of chloride concentration were monitored at four (4) observation points. These points coincide with screen positions of the test wells as shown in Table 7.4.3.

Table 7.4.3 OBSERVATION POINTS IN THE MODEL

Observation Point	Name of Test Well (depth)
Obs-1	LPS2-3 (100m)
Obs-2	LPS2-2 (200m)
Obs-3	LPS2-1 (300m)
Obs-4	LPS3-1 (300m)

Figure 7.4.7 to Figure 7.4.9 show changes of concentration over time. The saline water moves downward and reaches the bottom of Aquiclude-1 in 2.2 years since simulation started. After passing Aquiclude-1, the saline water intrudes in Aquifer-2 along the flow direction towards the low piezometric heads. In 7.1 years since simulation started, the fore-front of saline water reaches the center of piezometric depression in Aquifer-3. After 10 years, the contour of 2000mg/l reaches the center of piezometric depression.

Figure 7.4.10 shows changes of chloride concentration at the observation points. The chloride concentration increases from the first year since simulation started at Obs-1, then it rises steeply from the second to the forth year. By the sixth year the concentration shows high salinity

that is almost the same as seawater.

At Obs-2, the chloride concentration rises 4 years after the simulation started. It then increases gradually and reaches 13,000mg/l after 10 years simulation. At Obs-3 the concentration after 10 years is only 33mg/l. Saline water appears after 6 years of simulation.

The saline water appears at Obs-4 after 5 years simulation. Then the concentration increases constantly and it reaches 6,000mg/l by the tenth year.

(2) Source of Saline Water and Dispersivity

In order to identify the source of saline water, it was modeled that the sources of saline water be located at Manila Bay (x=3,y=2) and a marine pond (3,8). In this study it is assumed that the chloride concentrations of sea water and marine pond water are the same.

Figure 7.4.11 shows simulated chloride concentrations after 4.4 years and after 10 years. The longitudinal and transverse dispersivity is 7.0ft. The saline water from Manila Bay mainly goes downwards in Aquifer-1 and intrudes slowly towards inland in Aquifer-2. The forefront moves 200m in the lateral direction. In contrast, the saline water from the marine pond goes downward in Aquifer-1, and then moves as far as 1400m in Aquifer-2 and Aquifer-3, towards the center of piezometric depression. All these observations indicate the significant contribution of marine ponds and salty rivers in saline water intrusion.

The simulated chloride concentration using 33.0ft of longitudinal and transverse dispersivity is shown in Figure 7.4.12. The locations of saline water sources are the same as those in Figure 7.4.11. The result show that the saline water from both sea and marine pond disperses wider than the previous case. The saline water moves more downwards so that the contour of 2,000mg/l does not reach the center of piezometric depression. The saline water from the sea moves only 300m in the lateral direction even in this case. However, the simulated distribution of saline water is different from the actual distribution so that the dispersivity should be smaller than 33ft.

(3) Mechanism of Saline Water Intrusion

Above results show that the groundwater flow patterns greatly affect the movement of saline water. The marine ponds also substantially contribute to the saline water occurrence. To illustrate: If the source of saline water is only the sea, the distribution of saline water is very limited near the shoreline; in case the source of the saline water is assumed to be both the sea and marine ponds, the result shows good agreement with the actual saline water distribution and concentration.

7.4.3 Future Movement of Saline Water

The groundwater flow pattern in the future will be different from the present pattern because the locations and amount of discharge may be changed. Subsequently, the pattern of saline water occurrence may also be different.

The future movement of saline water will be controlled by the future pumpage in the area. It is easily predicted that if the existing depression of piezometric heads moves more inland, or a new bigger depression is formed in the more inland part, the saline water also moves deeper inland. Also, if deeper wells are constructed to extract from deeper aquifer, saline water may intrude more deeper portions.

According to the future water demand projections, the groundwater discharge in Las Piñas, Muntinlupa and Parañaque will decrease in the future, but the discharge in Cavite area will increase. Under scenario 1 the results of the groundwater flow simulation in Metro Manila show that large piezometric depressions will occur in Cavite, at the southern part of Las Piñas, and in Muntinlupa and Parañaque in the year 2010. This will cause further saline water intrusion in the area.

The simulation studies show that though the groundwater discharge in the coastal area is regulated, the piezometric depressions will remain in Muntinlupa and Parañaque. In this case saline water from Manila Bay will move towards the depressions, because the piezometric heads in the coastal area where saline water has already existed are higher than those in the inland area.

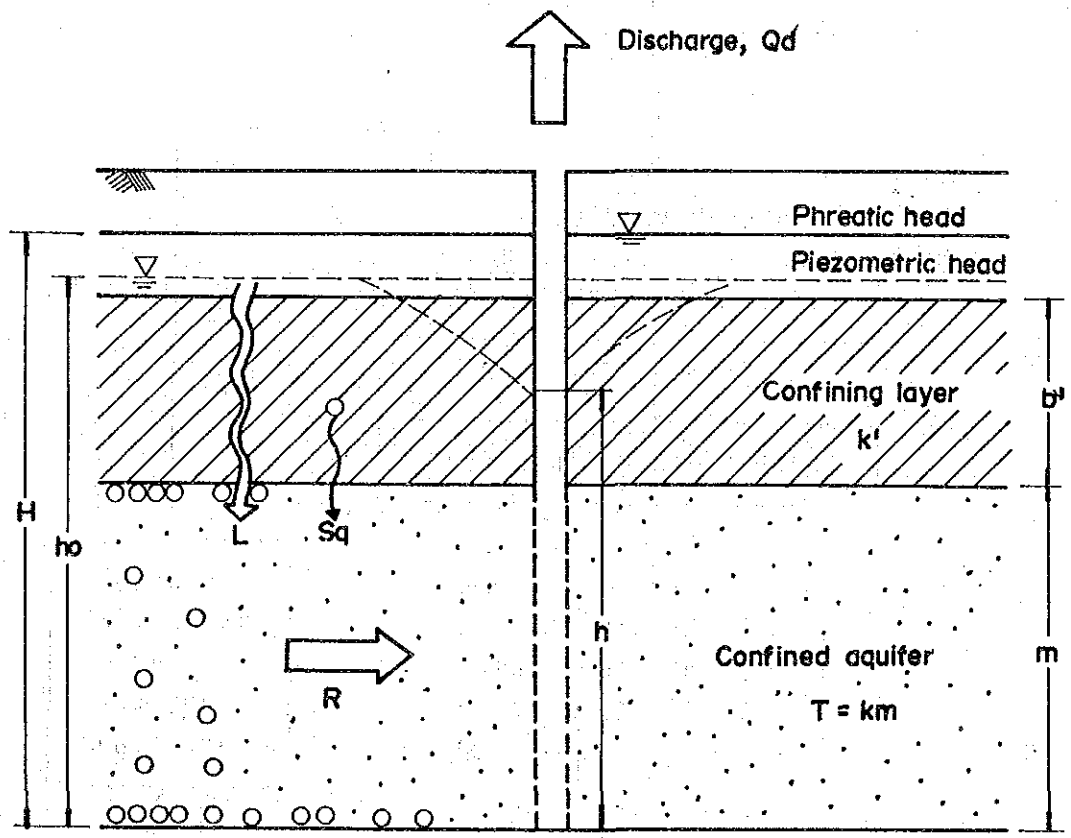

STUDY FOR THE GROUNDWATER DEVELOPMENT IN METRO MANILA JAPAN INTERNATIONAL COOPERATION AGENCY	FIGURE 7.1.1 SCHEMATIC CROSS-SECTION OF THE QUASI 3-DIMENSIONAL MODEL

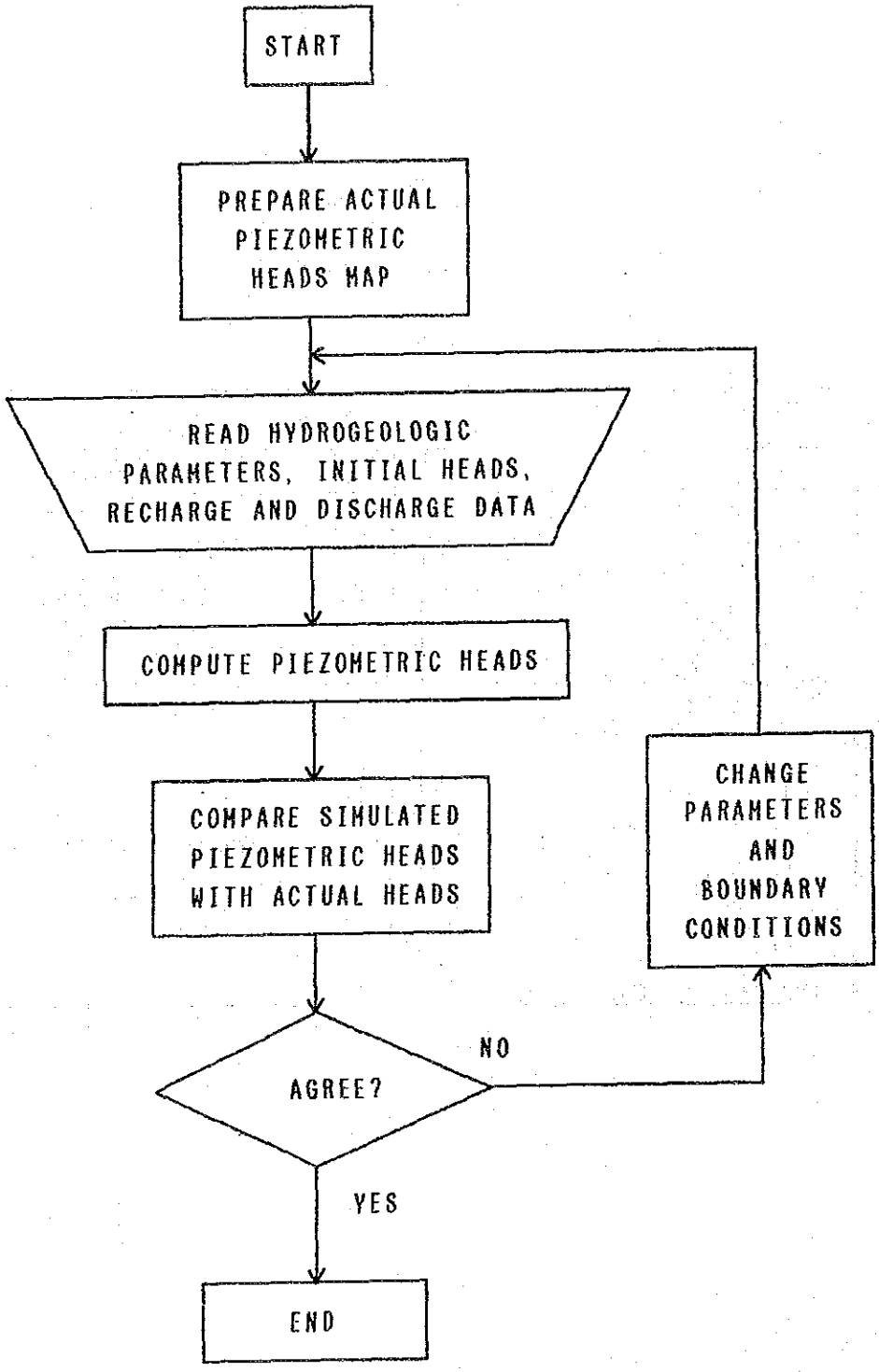

STUDY FOR THE GROUNDWATER DEVELOPMENT IN METRO MANILA	FIGURE 7.1.2 SIMPLIFIED FLOWCHART OF THE QUASI THREE-DIMENSIONAL FEM FLOW MODEL (Q3P)
JAPAN INTERNATIONAL COOPERATION AGENCY	

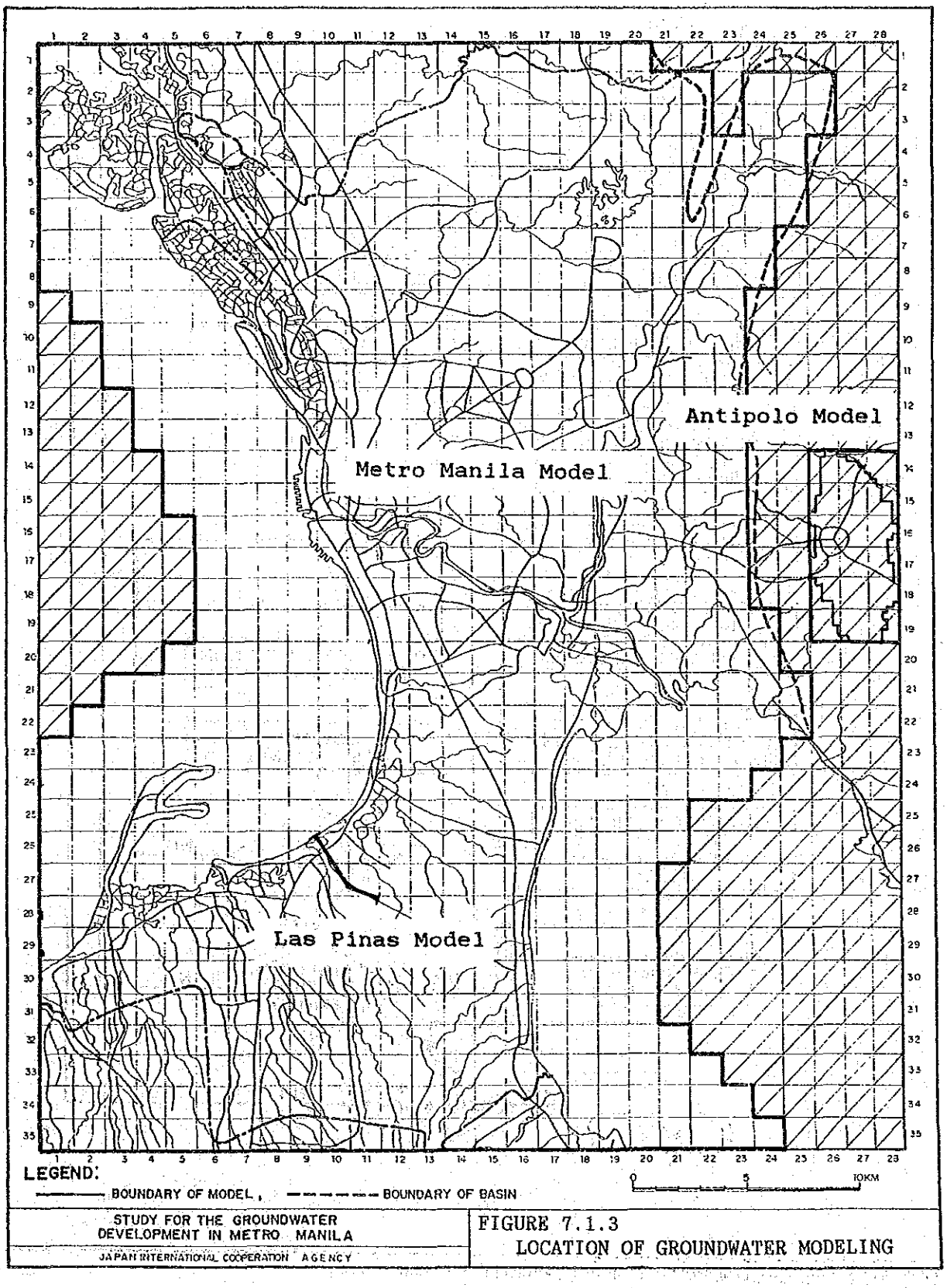

STUDY FOR THE GROUNDWATER DEVELOPMENT IN METRO MANILA

JAPAN INTERNATIONAL COOPERATION AGENCY

FIGURE 7.1.3
LOCATION OF GROUNDWATER MODELING

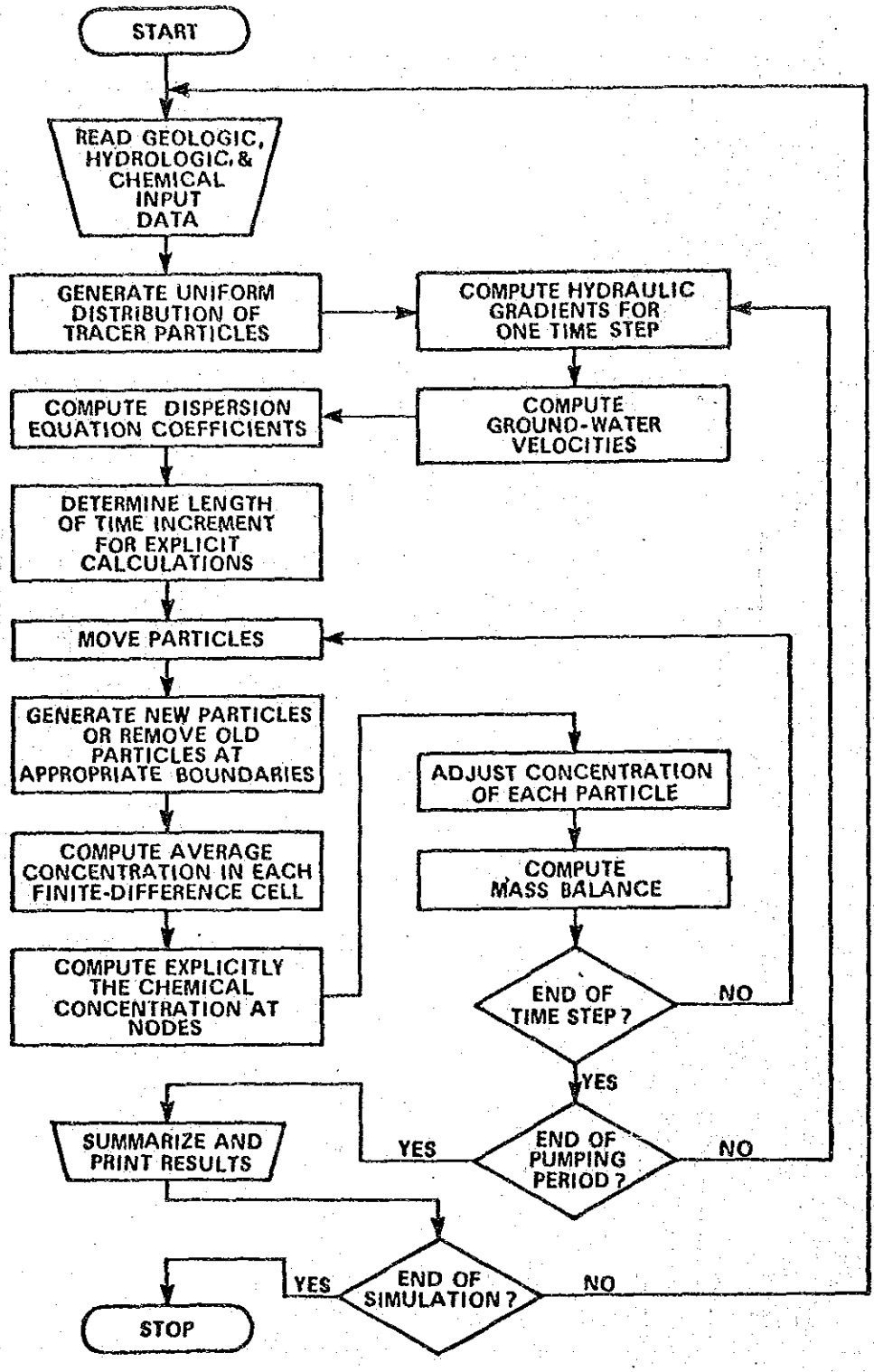

STUDY FOR THE GROUNDWATER DEVELOPMENT IN METRO MANILA	FIGURE 7.1.4 SIMPLIFIED FLOWCHART ILLUSTRATING THE MAJOR STEPS IN THE CALCULATION PROCEDURE
JAPAN INTERNATIONAL COOPERATION AGENCY	

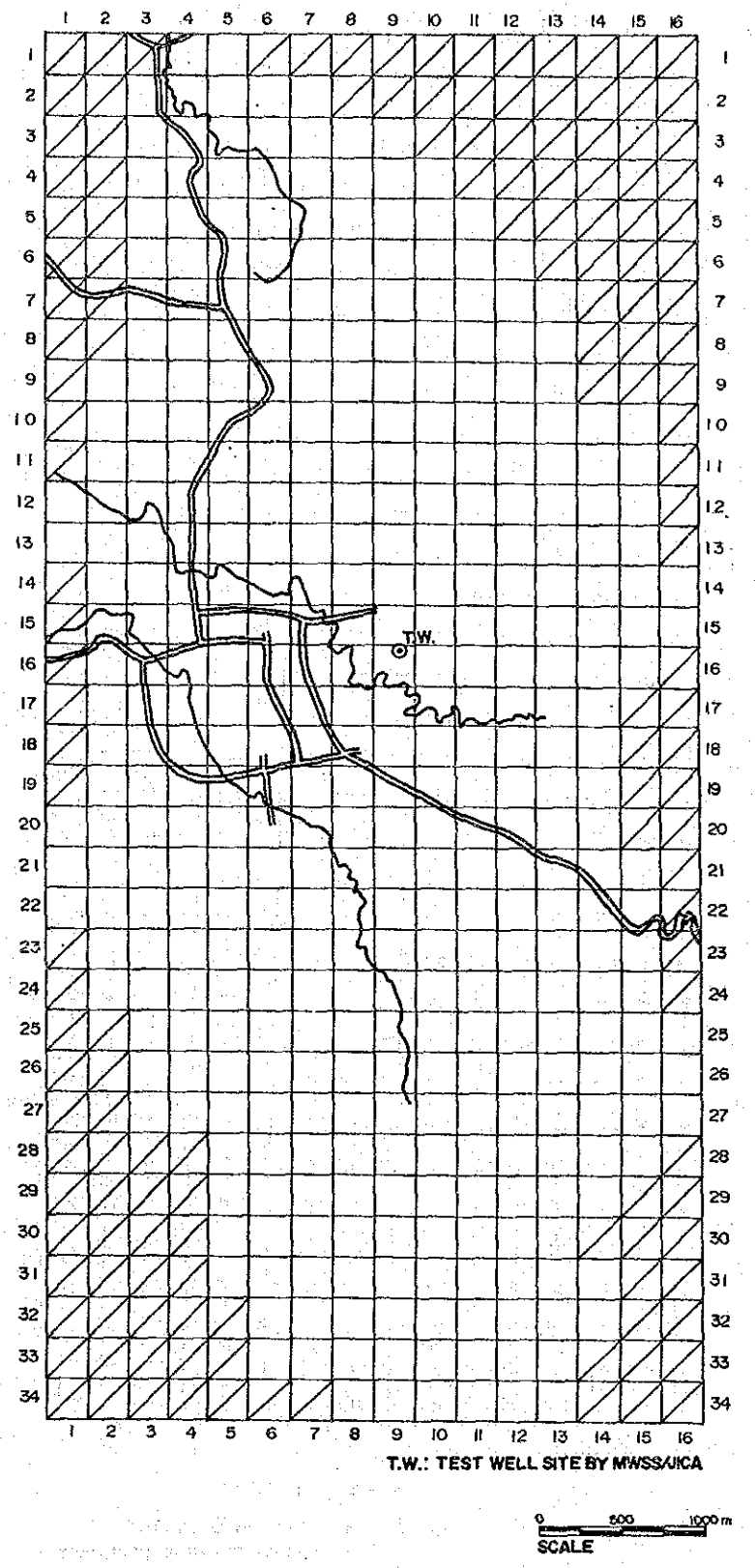

STUDY FOR THE GROUNDWATER DEVELOPMENT IN METRO MANILA	FIGURE 7.2.1 FINITE-ELEMENT GRID USED TO THE MODEL THE ANTIPOLO BASIN
JAPAN INTERNATIONAL COOPERATION AGENCY	

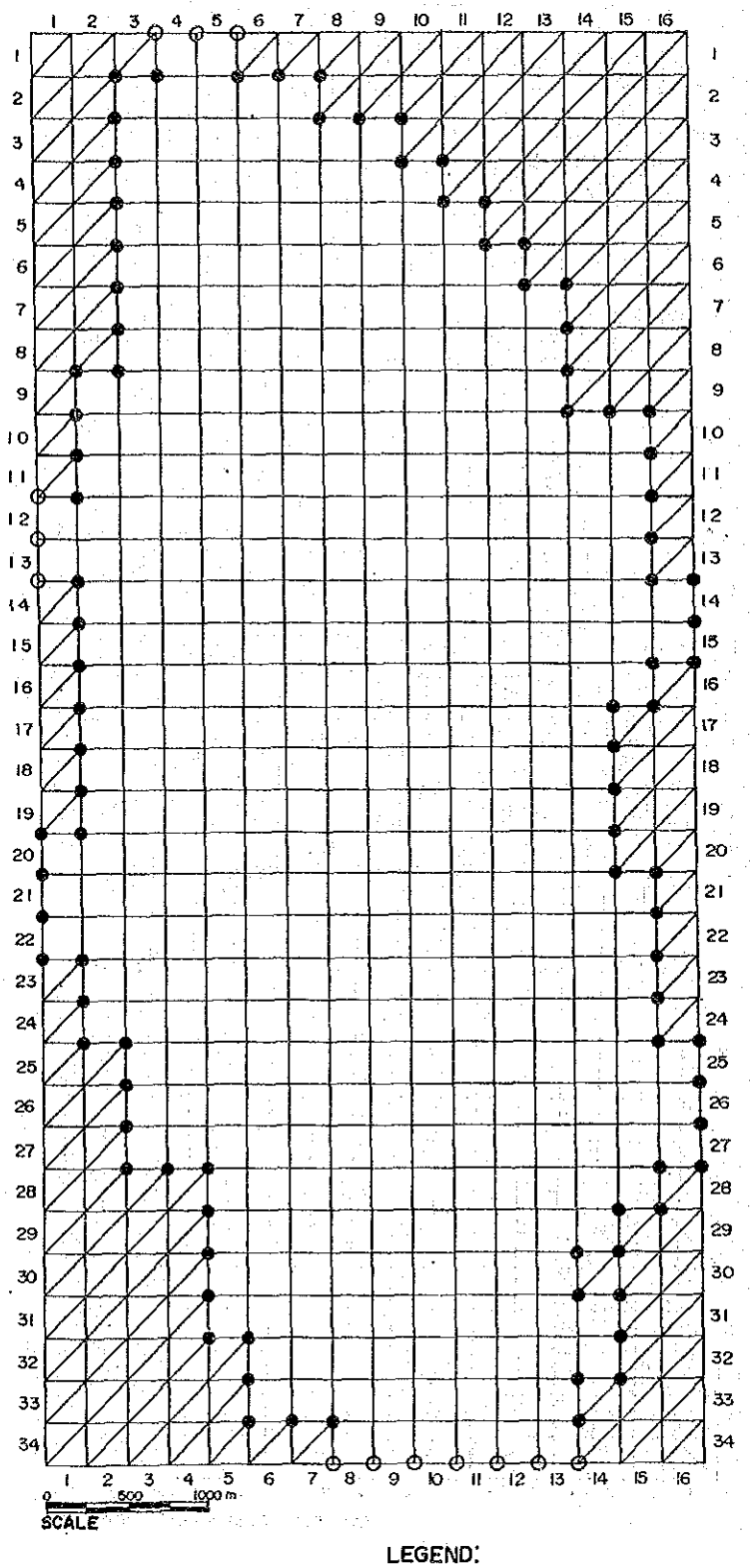

LEGEND:

- ● NO-FLOW BOUNDARY
- ○ CONSTANT-HEAD BOUNDARY

STUDY FOR THE GROUNDWATER DEVELOPMENT IN METRO MANILA

JAPAN INTERNATIONAL COOPERATION AGENCY

FIGURE 7.2.2

BOUNDARY CONDITIONS FOR THE ANTIPOLO GROUNDWATER BASIB MODEL

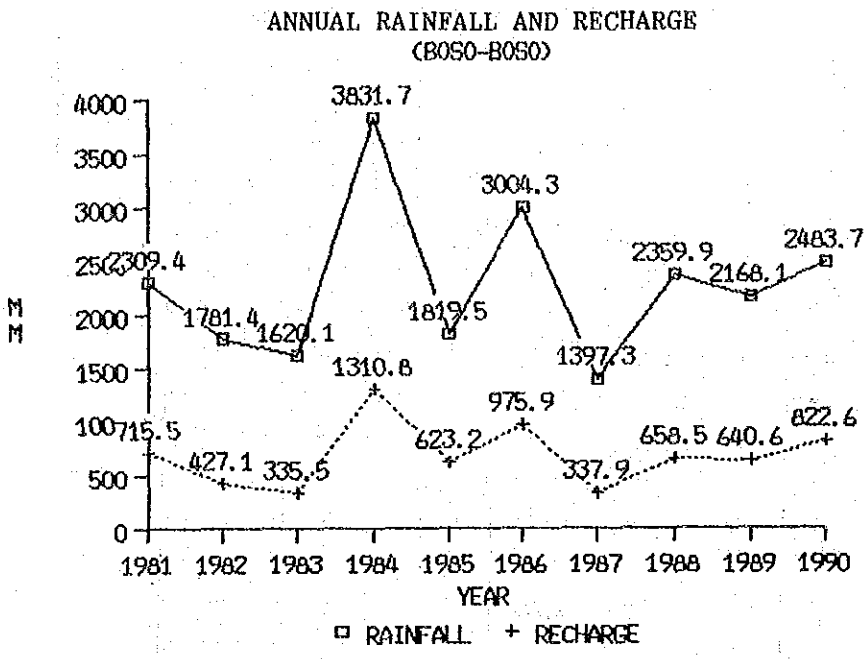

FIGURE 7.2.3
ANNUAL RAINFALL AND ESTIMATED RECHARGE AT BOSOBOSO-STATION

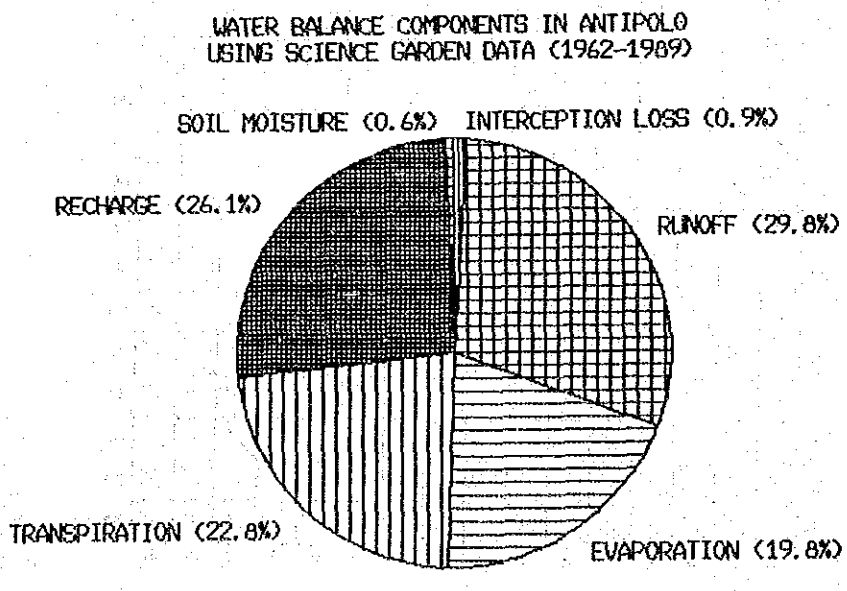

FIGURE 7.2.4
WATER BALANCE COMPONENTS IN ANTIPOLO BASIN
USING SCIENCE GARDEN DATA

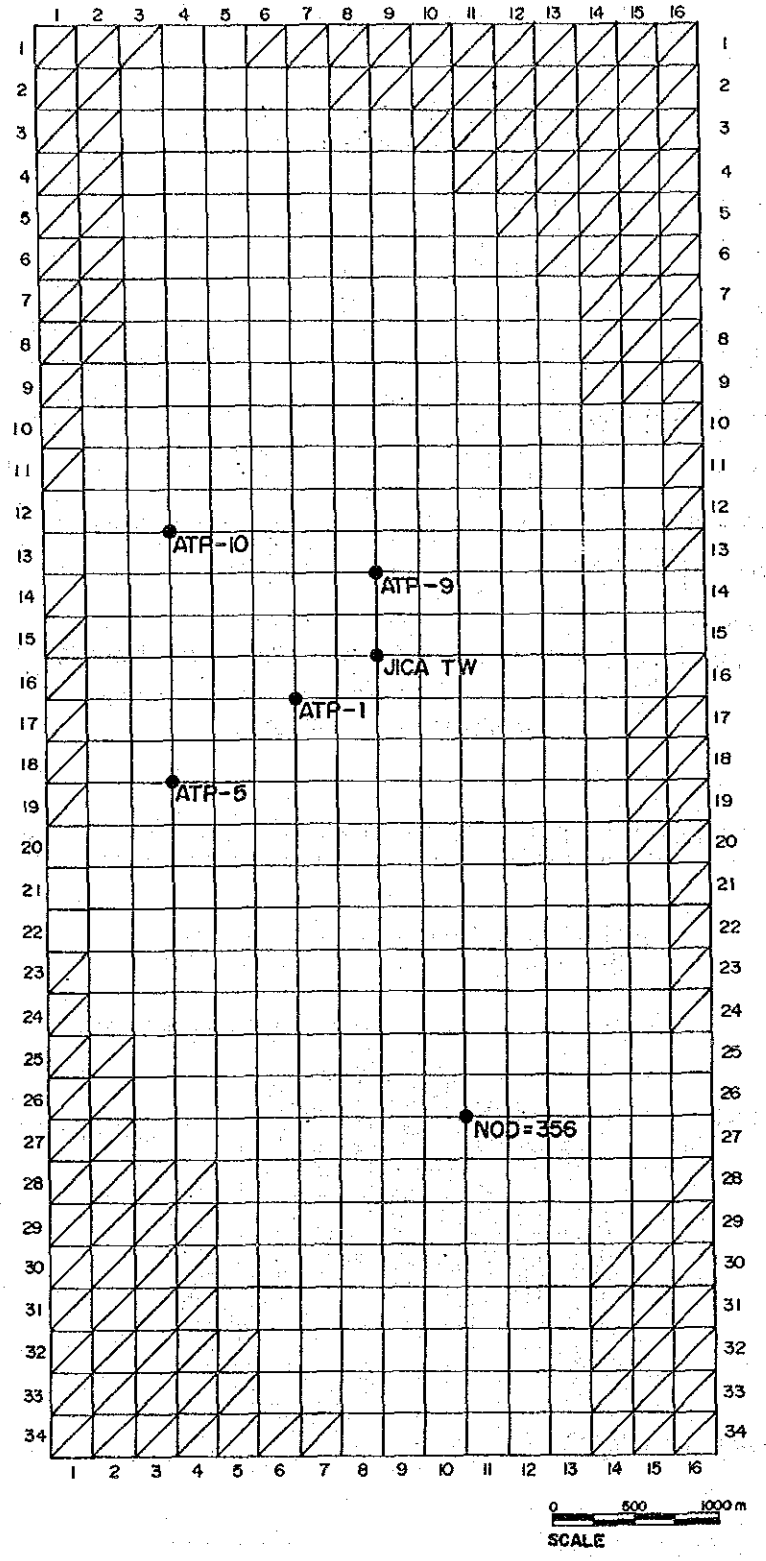

STUDY FOR THE GROUNDWATER DEVELOPMENT IN METRO MANILA	FIGURE 7.2.5 LOCATION OF OBSERVATION POINTS
JAPAN INTERNATIONAL COOPERATION AGENCY	

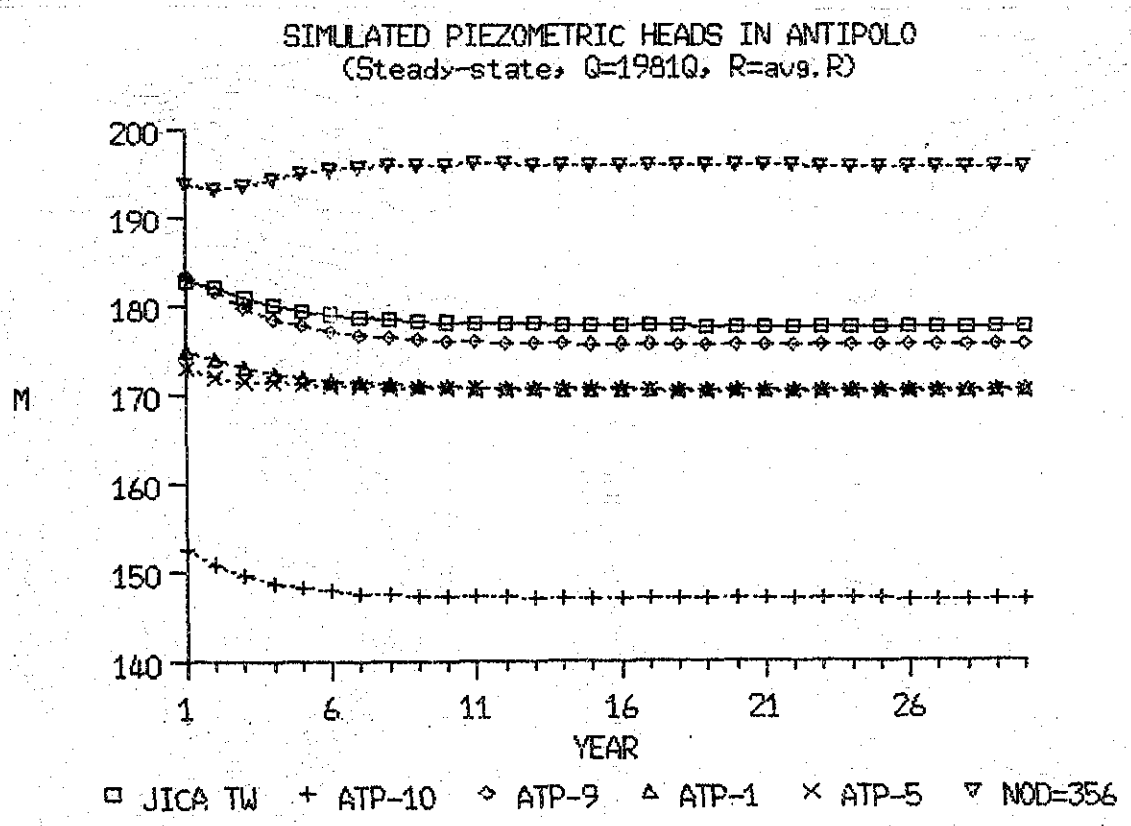

STUDY FOR THE GROUNDWATER DEVELOPMENT IN METRO MANILA	FIGURE 7.2.6
JAPAN INTERNATIONAL COOPERATION AGENCY	30-STEP STEADY-STATE CALCULATION TO MAKE INITIAL HEADS OF 1981

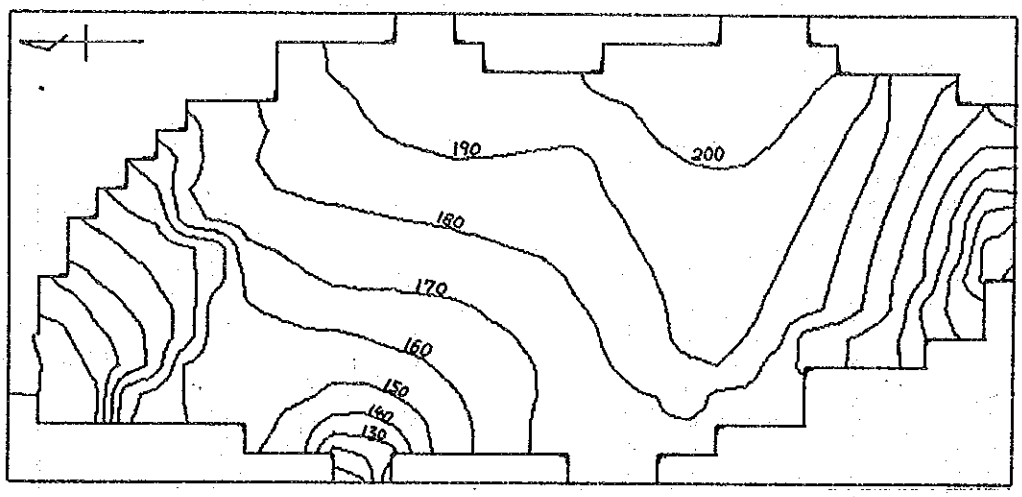

FIGURE 7.2.7 INITIAL PIEZOMETRIC HEADS OF 1981
FOR NONSTEADY-STATE SIMULATION

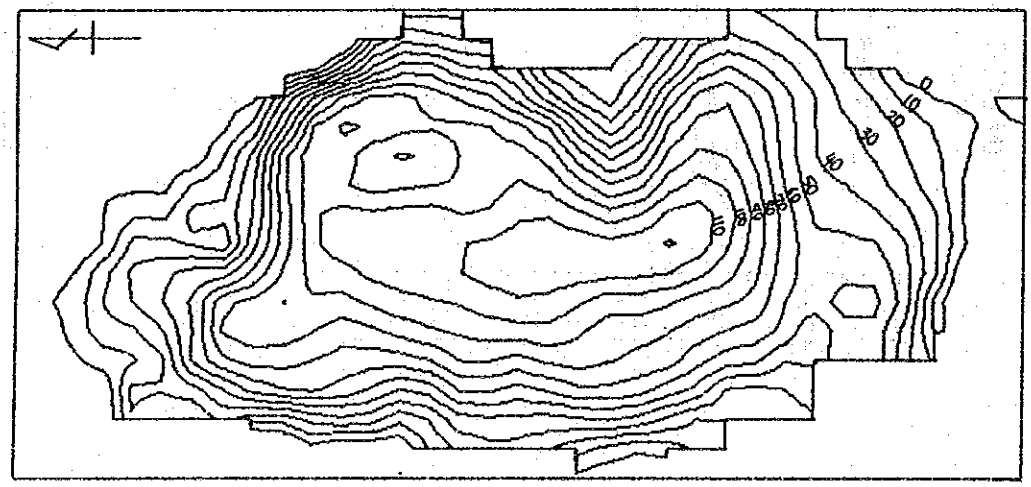

FIGURE 7.2.8
PIEZOMETRIC HEIGHTS FROM BOTTOM OF THE AQUIFER IN 1981

STUDY FOR THE GROUNDWATER DEVELOPMENT IN METRO MANILA	JAPAN INTERNATIONAL COOPERATION AGENCY

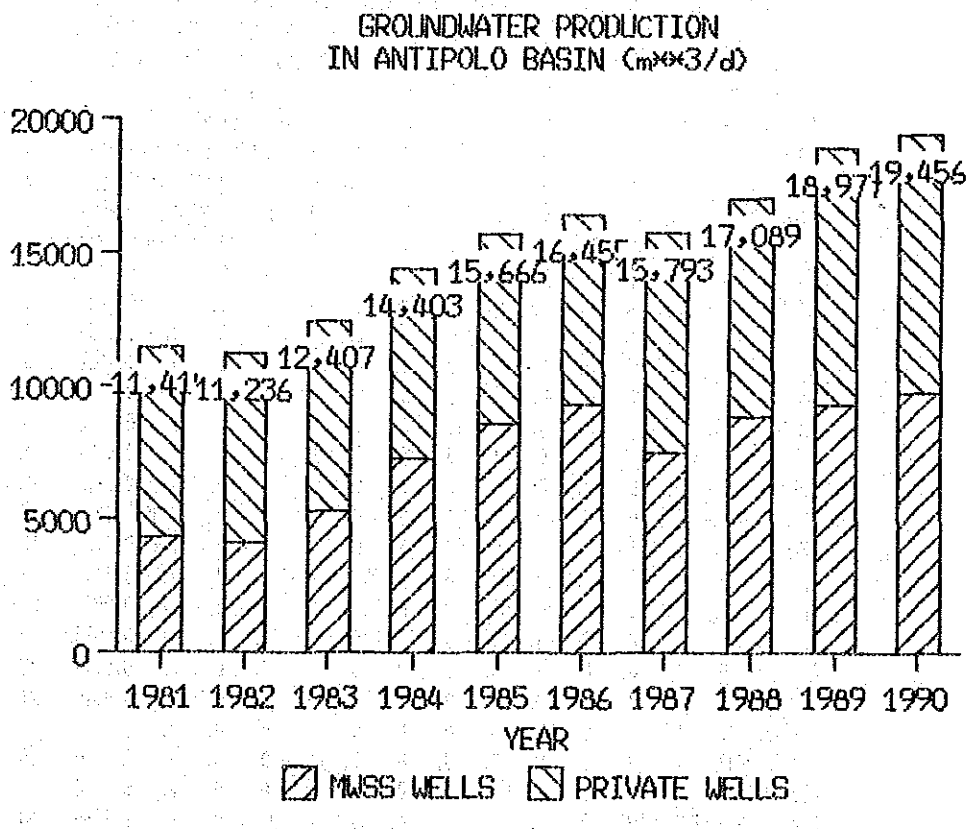

STUDY FOR THE GROUNDWATER DEVELOPMENT IN METRO MANILA	FIGURE 7.2.9 GROUNDWATER PRODUCTION IN THE ANTIPOLO BASIN (1981-1990)
JAPAN INTERNATIONAL COOPERATION AGENCY	

ATP Q MAP (m^3/d)
YEAR: 1981

1	2	3	4	5	6	7	8	9	10	11	12	13	14	15	16	
19999.	9999.	9999.	0.	0.	9999.	9999.	9999.	9999.	9999.	9999.	9999.	9999.	9999.	9999.	9999.	1
29999.	9999.	0.	0.	0.	0.	0.	9999.	9999.	9999.	9999.	9999.	9999.	9999.	9999.	9999.	2
39999.	9999.	0.	0.	0.	0.	0.	0.	0.	9999.	9999.	9999.	9999.	9999.	9999.	9999.	3
49999.	9999.	0.	0.	0.	0.	0.	0.	0.	0.	9999.	9999.	9999.	9999.	9999.	9999.	4
59999.	9999.	0.	0.	0.	0.	0.	0.	0.	0.	0.	9999.	9999.	9999.	9999.	9999.	5
69999.	9999.	0.	0.	0.	0.	0.	0.	0.	0.	0.	0.	9999.	9999.	9999.	9999.	6
79999.	9999.	0.	0.	0.	0.	0.	0.	0.	0.	0.	0.	0.	9999.	9999.	9999.	7
89999.	9999.	0.	0.	0.	0.	0.	0.	0.	0.	0.	0.	0.	9999.	9999.	9999.	8
99999.	0.	0.	0.	0.	0.	0.	0.	454.	0.	0.	0.	0.	9999.	9999.	9999.	9
109999.	0.	0.	0.	500.	0.	0.	0.	0.	0.	0.	0.	0.	0.	0.	9999.	10
119999.	0.	0.	0.	0.	0.	0.	0.	0.	0.	0.	0.	0.	0.	0.	9999.	11
12	0.	0.	0.	0.	0.	0.	0.	0.	0.	0.	0.	0.	0.	0.	9999.	12
13	0.	0.	0.	0.	0.	0.	0.	0.	0.	0.	0.	0.	0.	0.	9999.	13
149999.	0.	0.	0.	0.	0.	0.	0.	0.	0.	0.	0.	0.	0.	0.	0.	14
159999.	0.	0.	0.	0.	0.	0.	0.	0.	0.	0.	0.	0.	0.	0.	0.	15
169999.	0.	601.	0.	0.	0.	1377.	0.	0.	0.	0.	0.	0.	0.	0.	9999.	16
179999.	0.	0.	0.	0.	0.	0.	0.	0.	0.	0.	0.	0.	0.	9999.	9999.	17
189999.	0.	6.	0.	1636.	0.	1021.	0.	0.	0.	0.	0.	0.	0.	9999.	9999.	18
199999.	0.	0.	735.	0.	0.	0.	756.	0.	0.	1444.	0.	0.	0.	9999.	9999.	19
20	0.	0.	0.	0.	0.	0.	302.	0.	0.	252.	0.	1363.	0.	0.	9999.	20
21	0.	0.	0.	0.	0.	0.	302.	0.	0.	99.	0.	0.	0.	0.	9999.	21
22	0.	0.	0.	0.	0.	0.	0.	0.	0.	0.	0.	0.	0.	0.	9999.	22
239999.	0.	0.	0.	0.	0.	0.	0.	0.	0.	0.	0.	0.	0.	0.	9999.	23
249999.	0.	0.	0.	0.	0.	0.	0.	533.	0.	0.	0.	0.	0.	0.	9999.	24
259999.	9999.	0.	0.	0.	0.	0.	0.	0.	0.	0.	0.	0.	0.	0.	0.	25
269999.	9999.	0.	0.	0.	0.	0.	0.	0.	0.	0.	0.	0.	0.	0.	0.	26
279999.	9999.	0.	0.	0.	0.	0.	0.	0.	0.	0.	0.	0.	0.	0.	0.	27
289999.	9999.	9999.	9999.	0.	0.	0.	0.	0.	0.	0.	38.	0.	0.	0.	9999.	28
299999.	9999.	9999.	9999.	0.	0.	0.	0.	0.	0.	0.	0.	0.	0.	9999.	9999.	29
309999.	9999.	9999.	9999.	0.	0.	0.	0.	0.	0.	0.	0.	0.	9999.	9999.	9999.	30
319999.	9999.	9999.	9999.	0.	0.	0.	0.	0.	0.	0.	0.	0.	0.	9999.	9999.	31
329999.	9999.	9999.	9999.	9999.	0.	0.	0.	0.	0.	0.	0.	0.	0.	9999.	9999.	32
339999.	9999.	9999.	9999.	9999.	0.	0.	0.	0.	0.	0.	0.	0.	9999.	9999.	9999.	33
349999.	9999.	9999.	9999.	9999.	9999.	9999.	0.	0.	0.	0.	0.	0.	9999.	9999.	9999.	34
1	2	3	4	5	6	7	8	9	10	11	12	13	14	15	16	

TOTAL Q IN MODELED AREA = 11419.m^3/d

STUDY FOR THE GROUNDWATER DEVELOPMENT IN METRO MANILA	FIGURE 7.2.10 DISCHARGE MAP IN 1981
JAPAN INTERNATIONAL COOPERATION AGENCY	

ATP Q MAP (m^3/d)

YEAR: 1990

1	2	3	4	5	6	7	8	9	10	11	12	13	14	15	16	
19999.	9999.	9999.	0.	0.	9999.	9999.	9999.	9999.	9999.	9999.	9999.	9999.	9999.	9999.	9999.	1
29999.	9999.	0.	0.	0.	0.	0.	9999.	9999.	9999.	9999.	9999.	9999.	9999.	9999.	9999.	2
39999.	9999.	0.	0.	0.	0.	0.	0.	0.	9999.	9999.	9999.	9999.	9999.	9999.	9999.	3
49999.	9999.	0.	0.	0.	0.	0.	0.	0.	0.	9999.	9999.	9999.	9999.	9999.	9999.	4
59999.	9999.	0.	0.	0.	0.	0.	0.	0.	0.	0.	9999.	9999.	9999.	9999.	9999.	5
69999.	9999.	0.	0.	0.	0.	0.	0.	0.	0.	0.	0.	9999.	9999.	9999.	9999.	6
79999.	9999.	0.	0.	0.	681.	0.	0.	0.	0.	0.	0.	0.	9999.	9999.	9999.	7
89999.	9999.	0.	0.	0.	0.	0.	0.	0.	0.	0.	0.	0.	9999.	9999.	9999.	8
99999.	0.	0.	0.	0.	0.	0.	0.	454.	0.	0.	0.	0.	9999.	9999.	9999.	9
109999.	0.	0.	0.	500.	0.	0.	0.	0.	0.	0.	0.	0.	0.	0.	9999.	10
119999.	0.	0.	0.	0.	0.	27.	0.	0.	0.	0.	0.	0.	0.	0.	9999.	11
12	0.	0.	0.	0.	0.	0.	0.	0.	0.	0.	0.	0.	0.	0.	9999.	12
13	0.	0.	1571.	0.	0.	0.	0.	0.	0.	0.	0.	0.	0.	0.	9999.	13
149999.	27.	0.	0.	0.	0.	0.	1700.	1558.	0.	0.	0.	0.	0.	0.	0.	14
159999.	0.	0.	0.	0.	0.	0.	0.	0.	0.	0.	0.	0.	0.	0.	0.	15
169999.	0.	918.	0.	0.	0.	1076.	0.	0.	0.	0.	0.	0.	0.	0.	9999.	16
179999.	0.	0.	0.	1370.	0.	0.	0.	0.	0.	0.	0.	0.	0.	9999.	9999.	17
189999.	0.	6.	0.	1636.	0.	881.	0.	0.	0.	0.	0.	0.	0.	9999.	9999.	18
199999.	0.	0.	509.	0.	0.	0.	377.	0.	0.	1444.	0.	0.	0.	9999.	9999.	19
20	0.	0.	0.	0.	0.	36.	302.	0.	0.	252.	0.	1363.	0.	0.	9999.	9999.	20
21	0.	0.	0.	0.	0.	0.	302.	0.	0.	99.	0.	0.	0.	0.	0.	9999.	21
22	0.	0.	0.	0.	0.	648.	0.	0.	0.	0.	0.	0.	0.	0.	0.	9999.	22
239999.	0.	0.	0.	0.	0.	0.	0.	0.	0.	0.	0.	0.	0.	0.	0.	9999.	23
249999.	0.	0.	0.	0.	0.	0.	0.	0.	533.	0.	0.	0.	0.	0.	0.	9999.	24
259999.	9999.	0.	0.	0.	0.	0.	0.	0.	0.	0.	0.	0.	0.	0.	0.	0.	25
269999.	9999.	0.	0.	0.	0.	0.	0.	0.	0.	0.	0.	0.	0.	0.	0.	0.	26
279999.	9999.	0.	0.	0.	0.	0.	0.	0.	0.	0.	0.	0.	0.	0.	0.	0.	27
289999.	9999.	9999.	9999.	0.	0.	0.	0.	0.	0.	5.	45.	0.	0.	0.	9999.	28
299999.	9999.	9999.	9999.	0.	0.	0.	0.	0.	0.	0.	0.	0.	0.	9999.	9999.	29
309999.	9999.	9999.	9999.	0.	0.	0.	0.	0.	0.	0.	0.	0.	9999.	9999.	9999.	30
319999.	9999.	9999.	9999.	0.	0.	0.	0.	0.	0.	0.	1134.	0.	0.	9999.	9999.	31
329999.	9999.	9999.	9999.	9999.	0.	0.	0.	0.	0.	0.	0.	0.	0.	9999.	9999.	32
339999.	9999.	9999.	9999.	9999.	0.	0.	0.	0.	0.	0.	0.	0.	9999.	9999.	9999.	33
349999.	9999.	9999.	9999.	9999.	9999.	9999.	0.	0.	0.	0.	0.	0.	9999.	9999.	9999.	34
1	2	3	4	5	6	7	8	9	10	11	12	13	14	15	16	

TOTAL Q IN MODELED AREA = 19454.m^3/d

STUDY FOR THE GROUNDWATER DEVELOPMENT IN METRO MANILA	FIGURE 7.2.11 DISCHARGE MAP IN 1990
JAPAN INTERNATIONAL COOPERATION AGENCY	

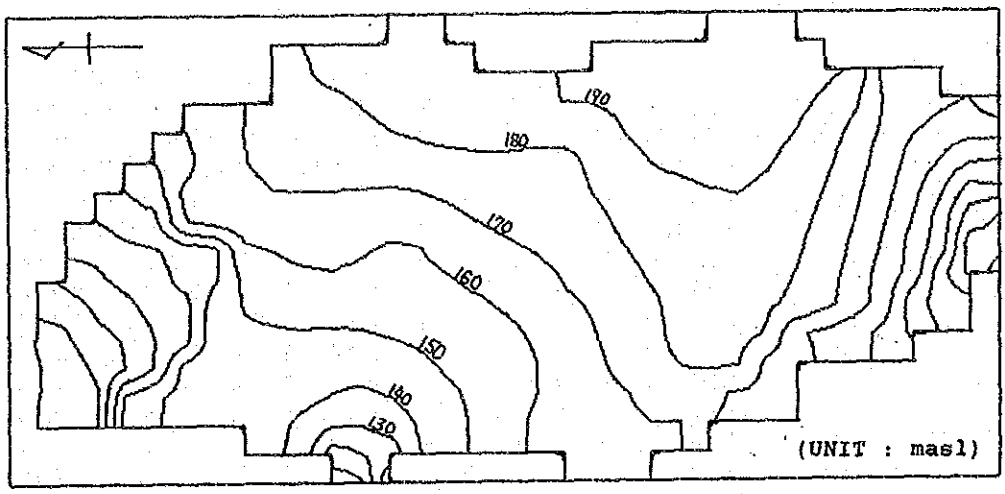

FIGURE 7.2.12
SIMULATED PIEZOMETRIC HEADS IN 1990

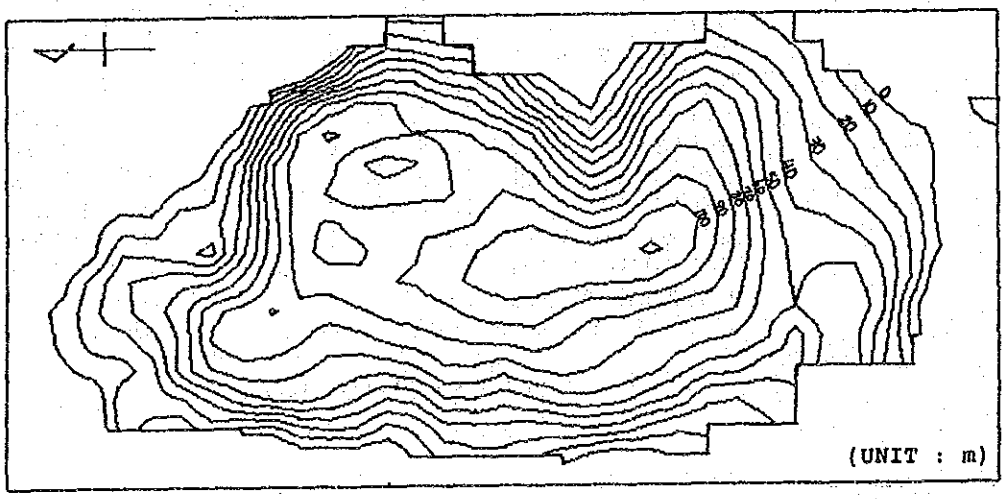

FIGURE 7.2.13 SIMULATED PIEZOMETRIC HEIGHTS FROM BOTTOM OF THE AQUIFER IN 1990

STUDY FOR THE GROUNDWATER DEVELOPMENT IN METRO MANILA	JAPAN INTERNATIONAL COOPERATION AGENCY

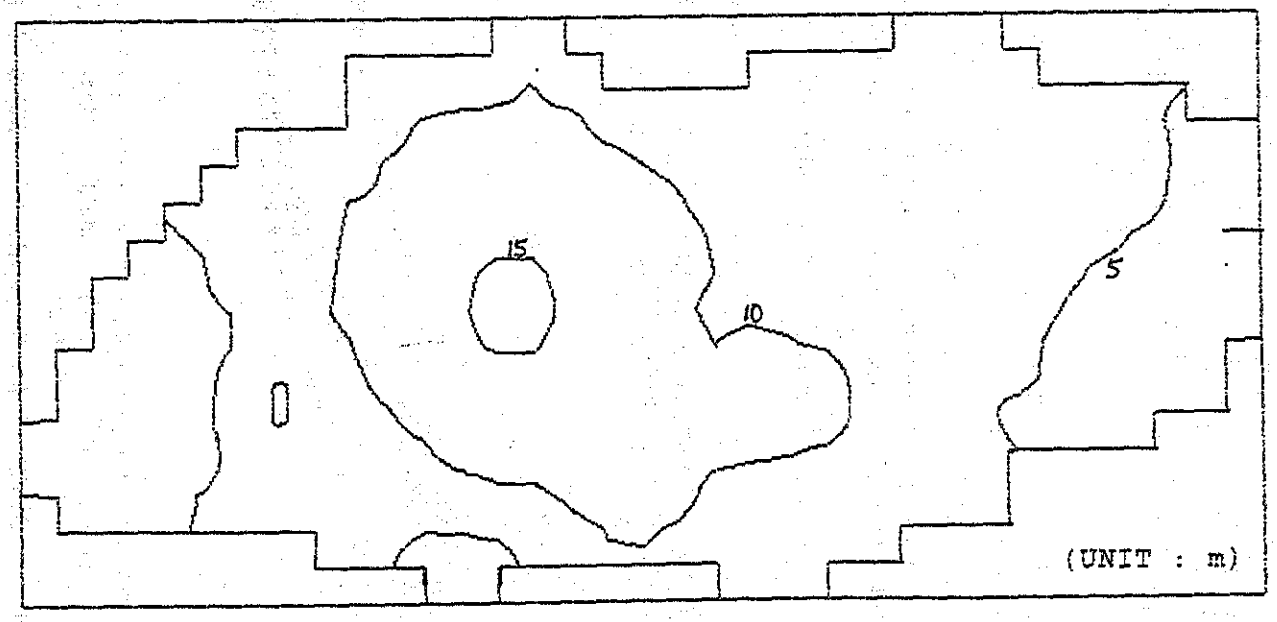

STUDY FOR THE GROUNDWATER DEVELOPMENT IN METRO MANILA	FIGURE 7.2.14 SIMULATED DRAWDOWN FROM 1981 TO 1990
JAPAN INTERNATIONAL COOPERATION AGENCY	

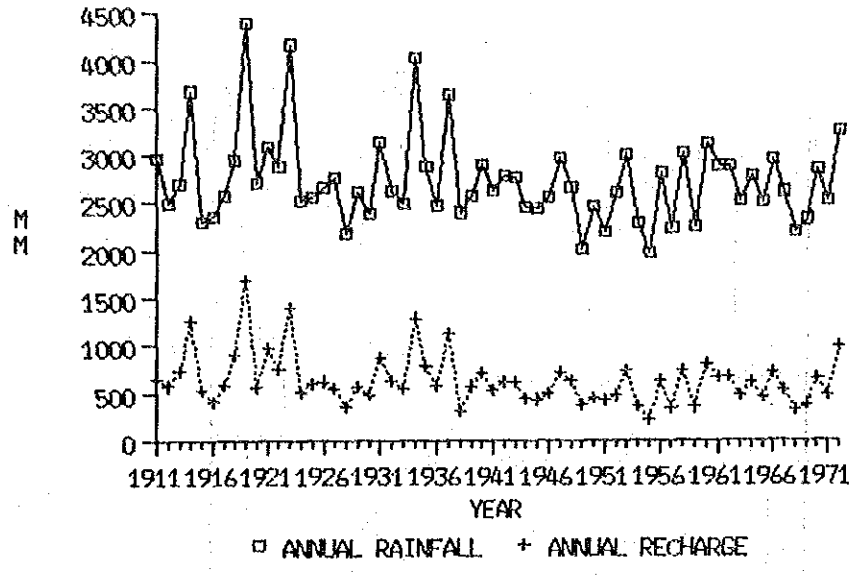

FIGURE 7.2.15
ANNUAL RAINFALL AND ESTIMATED RECHARGE IN ANTIPOLO USING SUMULONG STATION'S DATA (1911-1972)

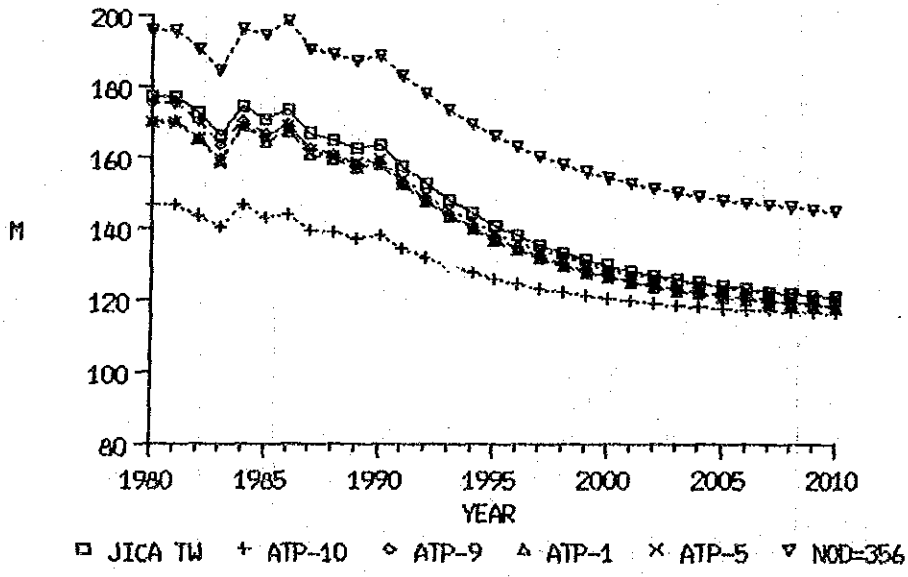

FIGURE 7.2.16
SIMULATED PIEZOMETRIC HEADS (Discharge from 1991 to 2010 = Discharge of 1990)

STUDY FOR THE GROUNDWATER DEVELOPMENT IN METRO MANILA	JAPAN INTERNATIONAL COOPERATION AGENCY

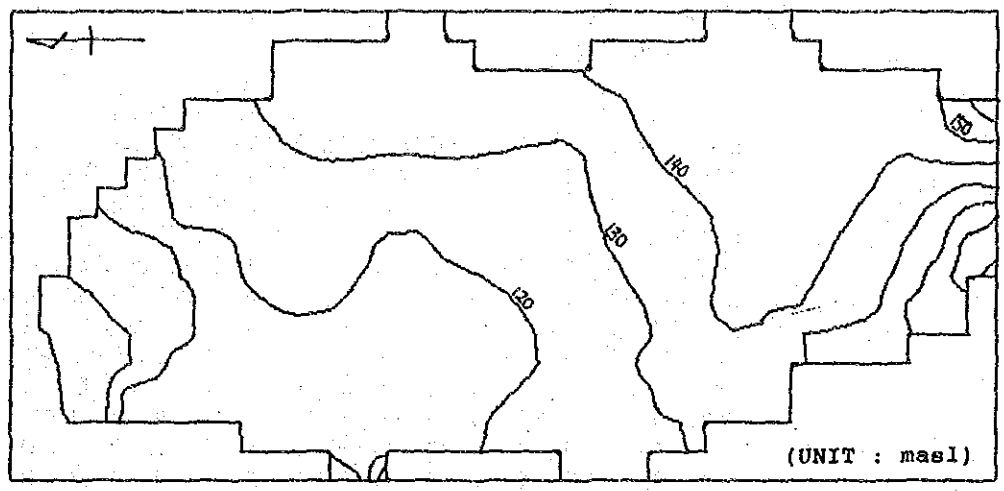

FIGURE 7.2.17
SIMULATED PIEZOMETRIC HEADS IN 2010 (Discharge from 1991 to 2010 = Discharge of 1990)

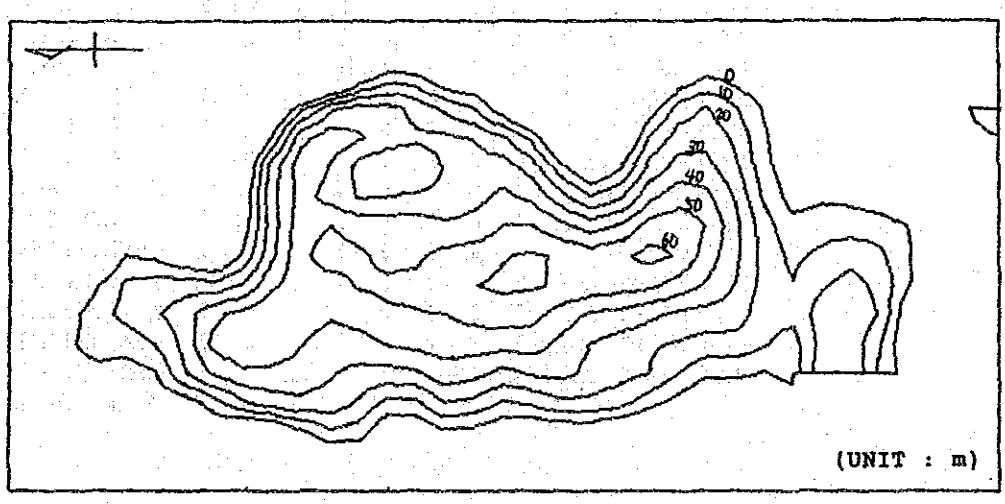

FIGURE 7.2.18 8
SIMULATED PIEZOMETRIC HEIGHTS FROM BOTTOM OF THE AQUIFER 2010 IN 2010 (Discharge from 1991 to 2010 = Discharge of 1990)

ATP Q MAP (m^3/d)

YEAR: 1991

1	2	3	4	5	6	7	8	9	10	11	12	13	14	15	16	
19999.	9999.	9999.	0.	0.	9999.	9999.	9999.	9999.	9999.	9999.	9999.	9999.	9999.	9999.	9999.	1
29999.	9999.	0.	0.	0.	0.	0.	9999.	9999.	9999.	9999.	9999.	9999.	9999.	9999.	9999.	2
39999.	9999.	0.	0.	0.	0.	0.	0.	0.	9999.	9999.	9999.	9999.	9999.	9999.	9999.	3
49999.	9999.	0.	0.	0.	0.	0.	0.	0.	0.	9999.	9999.	9999.	9999.	9999.	9999.	4
59999.	9999.	0.	0.	0.	0.	0.	0.	0.	0.	0.	9999.	9999.	9999.	9999.	9999.	5
69999.	9999.	0.	0.	0.	0.	0.	0.	0.	0.	0.	0.	9999.	9999.	9999.	9999.	6
79999.	9999.	0.	0.	0.	681.	0.	0.	0.	0.	0.	0.	0.	9999.	9999.	9999.	7
89999.	9999.	0.	0.	0.	0.	0.	0.	0.	0.	0.	0.	0.	9999.	9999.	9999.	8
99999.	0.	0.	0.	0.	0.	0.	0.	454.	0.	0.	0.	0.	9999.	9999.	9999.	9
109999.	0.	0.	0.	500.	0.	0.	0.	0.	0.	0.	0.	0.	0.	0.	9999.	10
119999.	0.	0.	0.	0.	0.	27.	0.	0.	0.	0.	0.	0.	0.	0.	9999.	11
12 0.	0.	0.	0.	0.	0.	0.	0.	0.	0.	0.	0.	0.	0.	0.	9999.	12
13 0.	0.	0.	1778.	0.	0.	0.	0.	[830.]	0.	0.	0.	0.	0.	0.	9999.	13
149999.	27.	0.	0.	0.	0.	[830.]	1907.	1765.	0.	0.	0.	0.	0.	0.	0.	14
159999.	0.	0.	0.	0.	0.	0.	0.	0.	0.	0.	0.	0.	0.	0.	0.	15
169999.	0.	1125.	0.	0.	0.	1490.	0.	0.	0.	0.	0.	0.	0.	0.	9999.	16
179999.	0.	0.	0.	1577.	0.	[830.]	0.	0.	0.	0.	0.	0.	0.	9999.	9999.	17
189999.	0.	6.	0.	1636.	0.	1088.	[830.]	0.	0.	0.	0.	0.	0.	9999.	9999.	18
199999.	0.	0.	716.	0.	0.	0.	0.	584.	0.	0.	1444.	0.	0.	9999.	9999.	19
20 0.	0.	0.	0.	0.	36.	[1132.]	[830.]	0.	252.	0.	1363.	0.	0.	9999.	9999.	20
21 0.	0.	0.	0.	0.	0.	302.	[830.]	0.	99.	0.	0.	0.	0.	0.	9999.	21
22 0.	0.	0.	0.	0.	648.	0.	0.	0.	0.	0.	0.	0.	0.	0.	9999.	22
239999.	0.	0.	0.	0.	0.	0.	0.	0.	0.	0.	0.	0.	0.	0.	9999.	23
249999.	0.	0.	0.	0.	0.	0.	0.	533.	0.	0.	0.	0.	0.	0.	9999.	24
259999.	9999.	0.	0.	0.	0.	0.	0.	0.	0.	0.	0.	0.	0.	0.	0.	25
269999.	9999.	0.	0.	0.	0.	0.	0.	0.	0.	0.	0.	0.	0.	0.	0.	26
279999.	9999.	0.	0.	0.	0.	0.	0.	0.	0.	0.	0.	0.	0.	0.	0.	27
289999.	9999.	9999.	9999.	0.	0.	0.	0.	0.	0.	5.	45.	0.	0.	0.	9999.	28
299999.	9999.	9999.	9999.	0.	0.	0.	0.	0.	0.	0.	0.	0.	0.	9999.	9999.	29
309999.	9999.	9999.	9999.	0.	0.	0.	0.	0.	0.	0.	0.	0.	9999.	9999.	9999.	30
319999.	9999.	9999.	9999.	0.	0.	0.	0.	0.	0.	0.	1134.	0.	0.	9999.	9999.	31
329999.	9999.	9999.	9999.	9999.	0.	0.	0.	0.	0.	0.	0.	0.	0.	9999.	9999.	32
339999.	9999.	9999.	9999.	9999.	0.	0.	0.	0.	0.	0.	0.	0.	9999.	9999.	9999.	33
349999.	9999.	9999.	9999.	9999.	9999.	9999.	0.	0.	0.	0.	0.	0.	9999.	9999.	9999.	34
1	2	3	4	5	6	7	8	9	10	11	12	13	14	15	16	

TOTAL Q IN MODELED AREA = 27334.m^3/d

□ : Location of New MWSS Wells

STUDY FOR THE GROUNDWATER DEVELOPMENT IN METRO MANILA	FIGURE 7.2.19 OPTIMAL DISCHARGE PLAN IN ANTIPOLO BASIN
JAPAN INTERNATIONAL COOPERATION AGENCY	

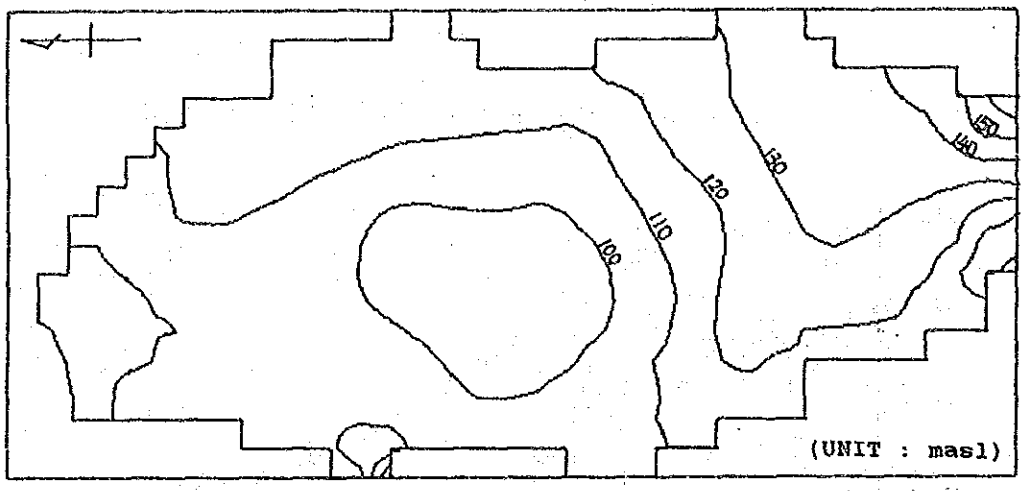

FIGURE 7.2.20
SIMULATED PIEZOMETRIC HEADS IN 2010 (Discharge from 1991 to 2010 = Optimal Plan)

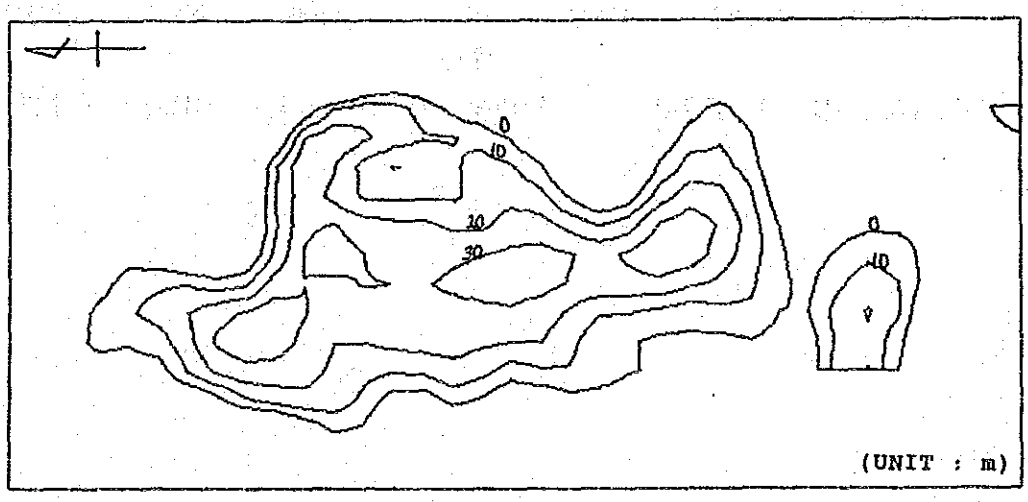

FIGURE 7.2.21
SIMULATED PIEZOMETRIC HEIGHTS FROM BOTTOM OF THE AQUIFER IN 2010 (Discharge from 1991 to 2010 = Optimal Plan)

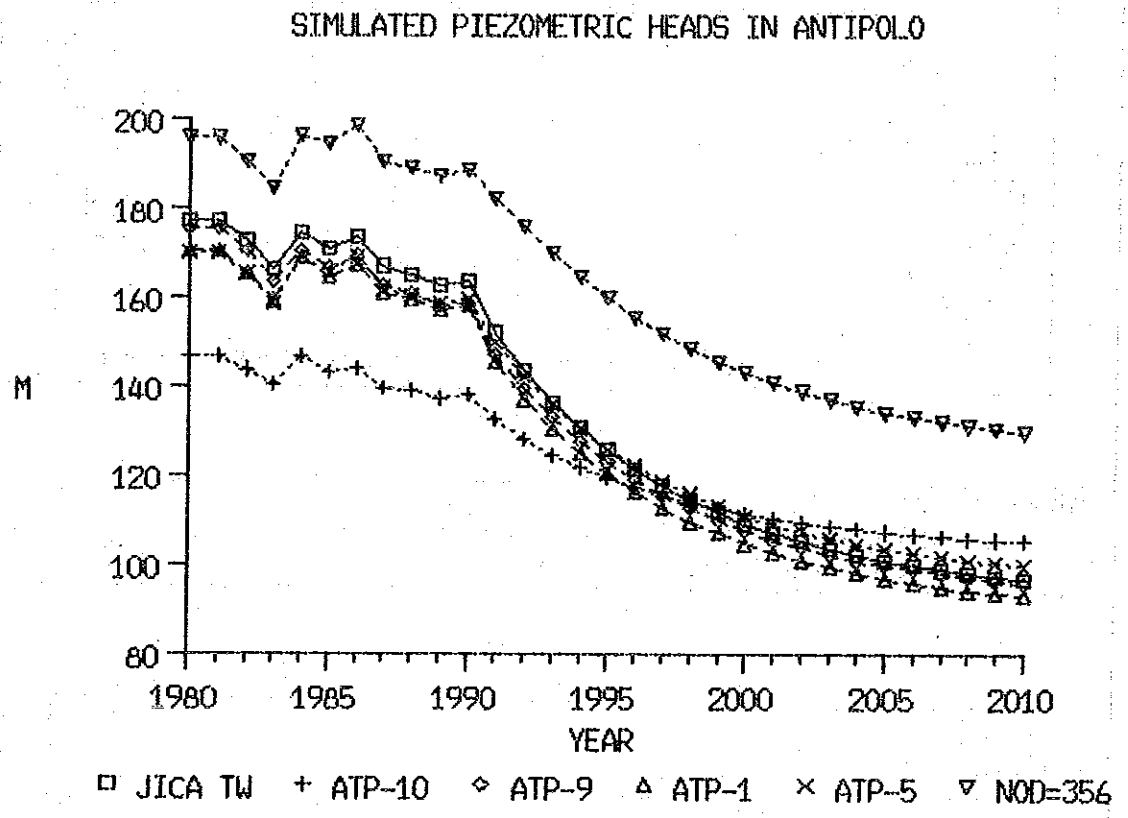

STUDY FOR THE GROUNDWATER DEVELOPMENT IN METRO MANILA	FIGURE 7.2.22
JAPAN INTERNATIONAL COOPERATION AGENCY	SIMULATED PIEZOMETRIC HEADS (Discharge from 1991 to 2010 = Optimal Plan)

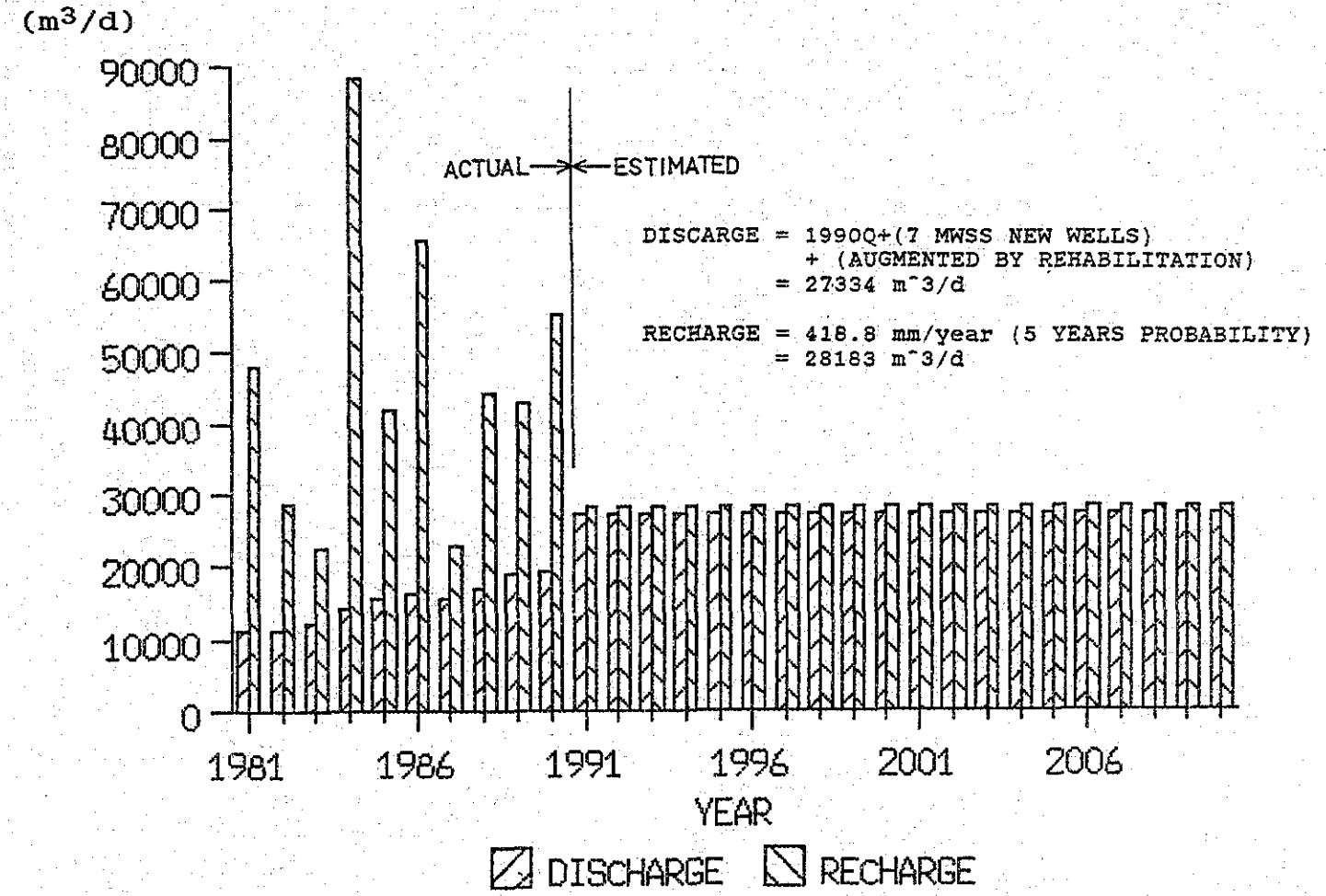

STUDY FOR THE GROUNDWATER DEVELOPMENT IN METRO MANILA	FIGURE 7.2.23 OPTIMAL DISCHARGE AND RECHARGE PLAN IN THE ANTIPOLO BASIN
JAPAN INTERNATIONAL COOPERATION AGENCY	